UiT
THE ARCTIC UNIVERSITY OF NORWAY

Faculty of Science and Technology

Department of Geoscience

Paleoceanographic development during the last deglaciation and Holocene, over the Bear Island slide scar, SW Barents Sea.

—

Ida Kristin Danielsen

GEO-3900 Master's thesis in Geology

February 2017

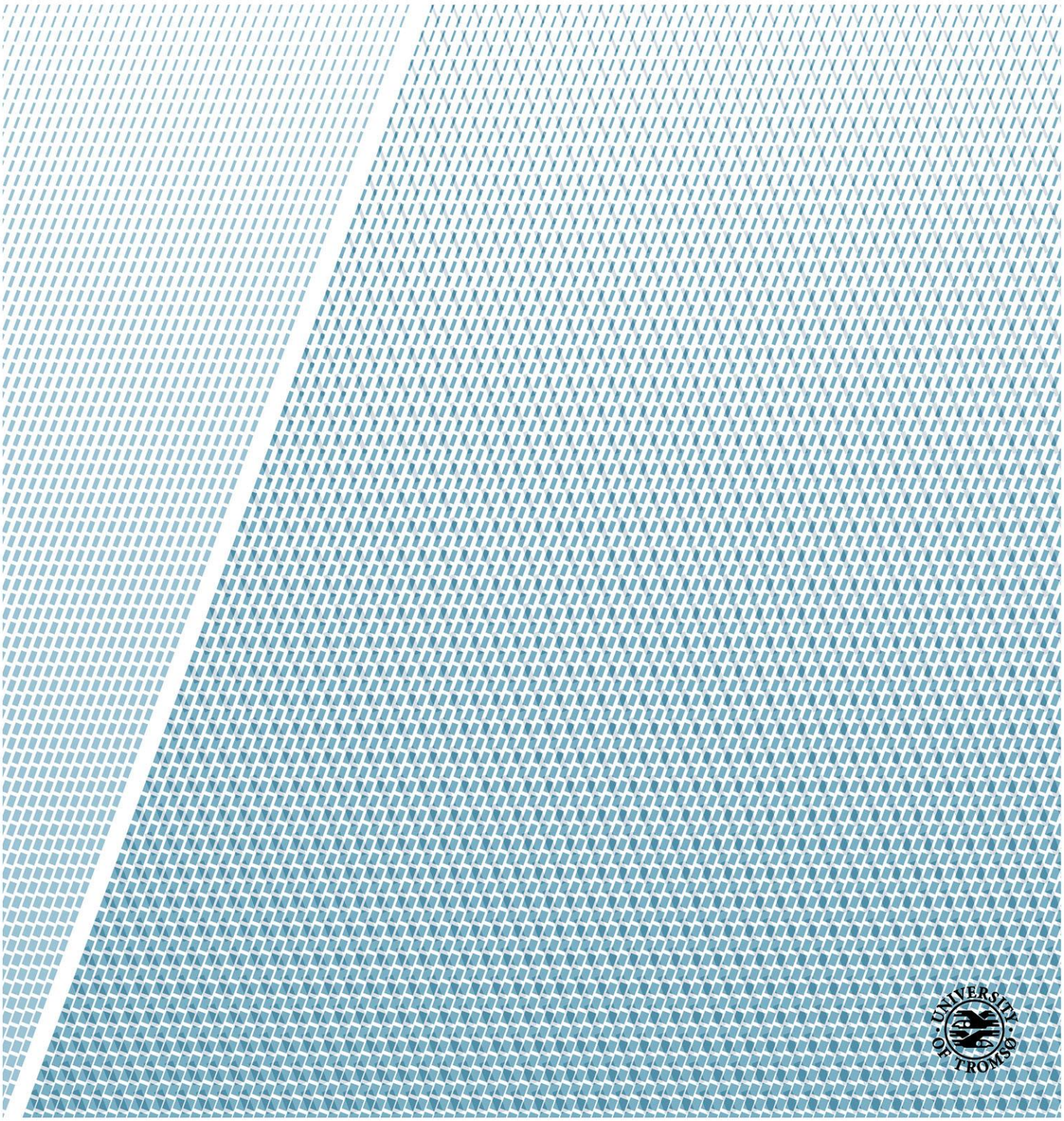

Abstract

The investigated sediment core HH13-243 GC is located under the present flow of the warm and saline Atlantic Water (AW), but close to, glaciated continental margins. The core site is situated in an area that is sensitive to changes and reflects the paleoceanography of the northernmost Norwegian Sea and the Western Barents Sea.

We investigated the changes in inflow of Atlantic water and the subsequent paleoceanographic development over the Bear Island slide scar, which is situated on the southern part of the Bear Island Through Mouth Fan. The results are based on planktic and benthic foraminiferal assemblages, stable isotopes and concentration and flux of IRD. An age model was established based on five AMS ^{14}C dates and the core were divided into six time intervals. The results indicate almost continuous presence of Atlantic water at the slope since ~15 500 cal. yr. BP. Heinrich event 1was characterised by warmer bottom water conditions than today and may reflect a 4-2 degree temperature change over a short time interval. Bølling- Allerød interstadial (15 400- 12 500 cal. yr. BP) was characterised by inflow of chilled Atlantic water with extensive sea ice cover. The transition from the Younger Dryas to the Early Holocene indicate an abrupt change in the planktic foraminiferal fauna, where warm water species replace the polar water species, and the Atlantic water dominate at the sea surface. The rest of the Holocene is characterized by mixing of Atlantic and Arctic water.

Forord

Først vil jeg rette en stor takk til min veileder Tine L. Rasmussen for muligheten til å skrive denne spennende masteroppgaven. Tusen takk for hjelp og gode råd. Det har vært en lang men spennende reise!

Jeg vil takke Trine Dahl, Ingvild Hald og Karina Monsen for all hjelp på laboratoriet og fine samtaler. Jeg vil også takke Kamila Sztybor og Mohammed Ezat for hjelp med å identifisere forskjellige arter og for alltid ha ett svar på spørsmål fra en frustrert student.

Jeg vil gjerne takke alle de fine folkene jeg har blitt kjent med i løpet av mine 7 år som student vet UiT, UNIS og UH Hilo. Det har virkelig vært den beste tiden i mitt liv! Det har til tider vært tungt men mest av alt utrulig morsomt med mange fine opplevelser.

Å spesielt takk til Ingrid, Silje, Kristina og Cathrine nå i innspurten, for alltid å ha tid til en stresset men engasjert Ida.

Til mine foreldre, TUSEN TAKK for all støtte og oppmuntring, hadde ikke klart dette uten dere. Vil også takke mine søsken for fine samtaler og avbrekk. Vil også rette en tanke til min lillebror, Ola og venninne Susann.

Til slutt vil jeg igjen bare si tusen hjertelig takk, nå venter ski og fjell!

Ida Kristin Danielsen

Tromsø, 1. februar 2017

Contents

1. Introduction

1.1. Objectives

The aim of this study is to gain a better understanding of the inflow of Atlantic water at greater depths, and the development of the paleoceanography at the study area from the latter part of the deglaciation until today. The results and reconstruction are based on a multi-proxy approach using foraminiferal and sedimentological records from a marine sediment core. The core was recovered from a water depth of 1448 m, from the Bear Island slide scar, which is a part of the continental slope of the southwester Barents Sea.

1.2. Background

During the last decade, several studies have been carried out to reconstruct the changes in the ocean circulation and climate of the Nordic and Barents Sea (Hald et al., 1989; Koç et al ., 1993; Hald and Aspeli, 1997; Slubowska-Woldengen et al., 2008). Furthermore, because of this, a coherent reconstruction of the area can give a more widely geographical and temporal scale of the paleoceanographic changes and document the changes in the different branches of the Atlantic Water inflow (Slubowska-Woldengen et al., 2008). The most widespread microfossil organism on the shelf areas of the Nordic and Barents Sea is the benthic foraminifera, while the planktonic foraminifera dominate the deeper sea. The foraminifera are dependent on several environmental parameters; there is a clear zonation between the faunal distributions. The faunal composition in the particular area reflects the location and movements of oceanic fronts and the food availability as much as the oceanographic conditions (e.g. Murray 1991; Slubowska-Woldengen et al., 2008). This master thesis is focusing on the reconstruction of changes in the bottom as well as the surface circulation of Atlantic Water on the continental slope of the southwestern Barents Sea during the last Deglaciation and Holocene. The purpose is to gain a better understanding of inflow of Atlantic Water at greater depths and examine the phasing and strength of the Atlantic Water flow at the study area. To address this, the study is based on the benthic and planktic foraminiferer species distribution, ice-rafted debris (IRD), lithology and stable isotopes and ^{14}C dates.

1.3.Study area

The location of the investigated sediment core are located under the present flow of the warm and saline Atlantic Water (AW) and beyond, but close to, glaciated continental margins. The core site is situated in an area that is sensitive to changes and reflects the paleoceanography of the northernmost Norwegian Sea and the southwestern Barents Sea (Figure 1).

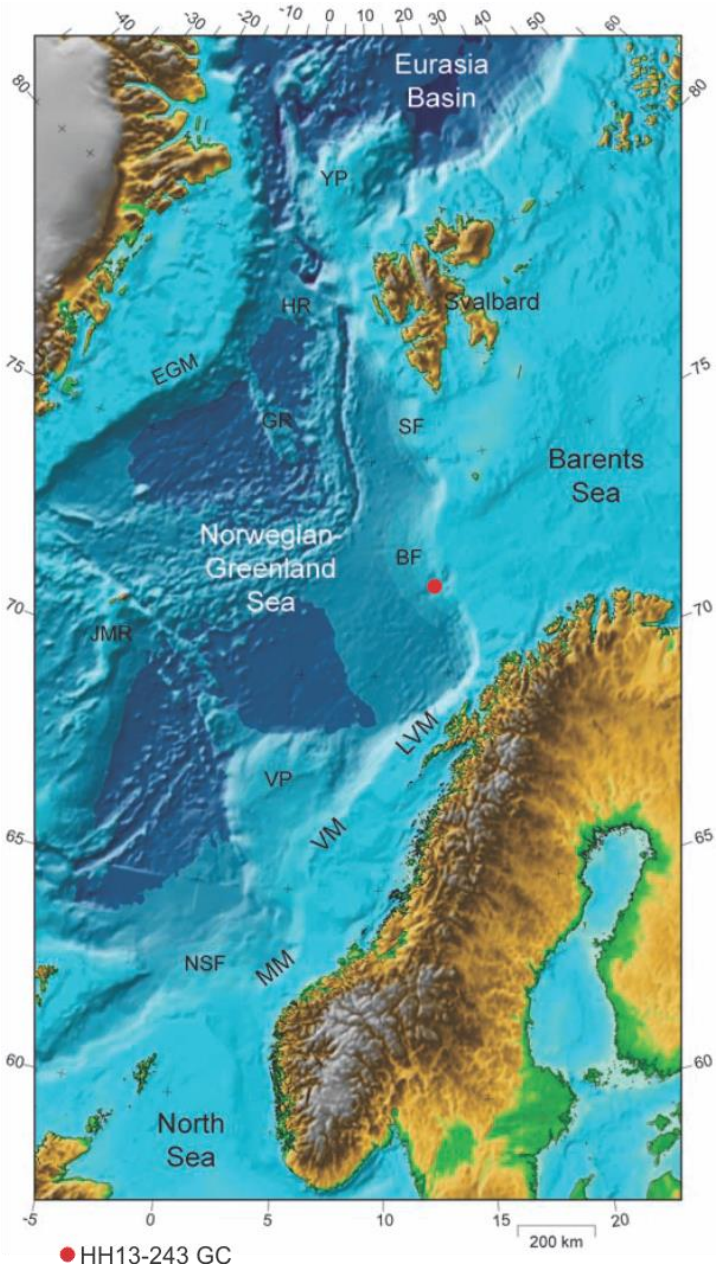

Figure 1: Overview map of the study area, SW Barents Sea and the norther Norwegian Sea. Core location of HH13-243 GC is indicated by a red circle. The figure is modified from Faleide et al. (2008).

The study is situated along the southwestern Barents Sea continental slope. The Barents Sea is an epicontinental sea and covers one of the widest continental shelves in the world (Vorren et al., 1998) of approximately 1,3 millions km^2 (Doré, 1995). The Bear Island Trough Mouth Fan is located in front of a large transverse through; the Bear Island Through which is the most distinctive formation in the western Barents Sea (Andreassen et al., 2008). The fan can be followed from the shelf break and down to water depths exceeding 3000 meters where it merges with the abyssal plain in the Lofoten Basin in the Norwegian Sea (Vorren et al., 1998). The Bear Island TMF has a width of about 250 km in the proximal part and around 440 km at greater water depths of 2200 and covers a total area of approximately 215 000 km^2 (Vorren et al., 1998).

The morphology of the fan is affected by the Bear Island slide scar in the southern part (Vorren et al., 1998), the core is collected from this area at 1448 m water depth. The slide scar is characterized by a bathymetric depression that is most pronounced on the upper slope and decreases gradually downslope to a water depth of around 2500 m and is up to 400 m deep (Laberg and Vorren, 1993).

1.4. Oceanographic and environmental setting

Warm Atlantic Water (AW) enters the Nordic Seas (Norwegian Sea, Greenland Sea and Iceland Sea) and Barents Sea in the east via the Norwegian Atlantic Current (NwAW), a continuation of the North Atlantic Current (NAC) (De Schepper et al., 2015).

The North Atlantic Current (NAC) (Figure2) that transport heat and salt northward to higher latitudes plays a big role for the climate in the region and is a part of the thermohaline circulation. The thermohaline circulation is driven by density differences between the water masses due to various temperatures and salinity (Broecker, 1991). The ocean circulation and the distribution of the different water masses is mainly determined by the bathymetry (Rudels, 1987; Pfirman et al., 1994; Slubowska-Woldengen et al., 2008). The major flow of the AW enters the Nordic Seas trough the Faeroe-Shetland Channel and follow the Norwegian continental slope to higher latitudes. Here a branch of the AW mixes with brackish water from the main land, and form the Norwegian costal current (Blindheim, 1987).

On its northward passage, the NwAC split into two, one part is entering the southern Barents Sea as the North Cape Current (NCaC), whereas the other follow the Barents Sea slope as the West-Spitsbergen Current (WSC) (Johannesen, 1986). The WSC enters the Arctic Ocean through the Fram Strait, and is considered to be the major current delivering heat and saline water to the Arctic Ocean (AAgaard and Greisman, 1975; Saloranata et al 2001). On its northward passage the AW loses heat and gets dense due to surface cooling, and at about 78°N it submerges the colder and less saline Arctic surface water (ASW), and follow the bathymetry of the western Svalbard slope (Slubowska-Woldengen et al., 2008). The bathymetry splits the WSC into three branches that's follow different bathymetrical paths (Manley, 1995).

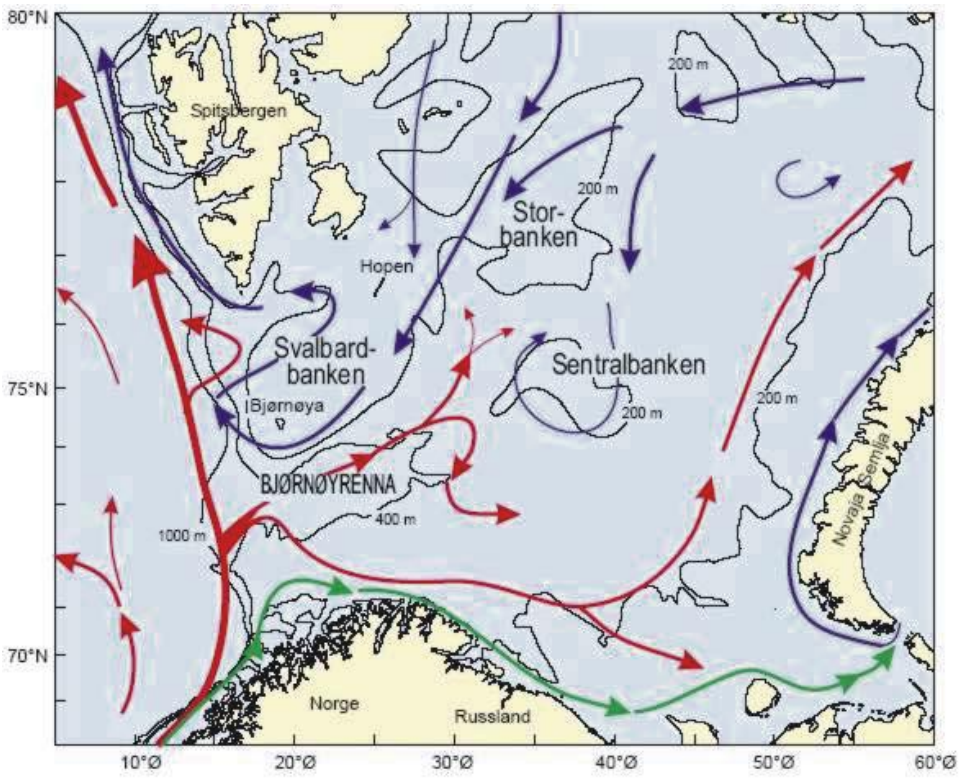

Figure 2: General circulation of the surface water masses in the Barents Sea. Red arrows: North Atlantic Water. Blue arrows: Arctic Water. Green arrows: Costal Water. (figure from Ingvaldsen et al., 2005)

Cool, Polar Water (PW) and sea ice are exported from the Arctic Ocean and enters the Nordic Seas in the west via the East Greenland Current (EGC) (Broecker, 1997; Saloranta et al., 2001), where a fraction of Polar Water is transported to the Barents Sea by the East Spitsbergen Current (ESC) (De Schepper et al., 2015). The strength and route of the EGC depends on the polar pack ice and fresh water from the Arctic Ocean and the atmospheric circulation (Denser et al., 2000).

1.5. Glacial history

Grounded ice sheets have covered the Barents Sea several times during the late Cenozoic. During these larger glaciations, the margin of the ice sheet reached out to the shelf edge, and the continental shelf and slope operated as a depocenter and prograded rapidly. During interglacials, the sedimentation rate decreased drastically, and the Barents Sea was altered to be a starved continental margin (Vorren et al. 1988).

1.5.1. LGM

At the late Late Weichelian maximum, an ice sheet covered the whole of the Barents Sea continental shelf extending to the shelf edge (Vorren et al., 2011). The ice drainage was concentrated in the Bear Island Ice Stream, which was fed by large source areas from the north-east and south. Two main ice streams merged with the Bear Island Ice Stream. In the east, an ice stream flowed into the White Sea through Kandalaksa Gulf. It is uncertain whether the ice stream continued south-eastwards or if it curved and contributing ice to the Bear Island Ice Stream (Vorren et al., 2011).

1.5.2. Deglaciation

Deglaciation began whit significant retreat of the ice margin in the southern Barents Sea.
The glacial morphology indicate spatial and temporal variations in the ice dynamics, where there are evidence of both active ice streaming and frozen-bed conditions at both maximal glacial extent and during phases of deglaciation (Winsborrow et al., 2010).
A grounding zone wedge in the Bear Island Through indicated retreat and subsequent readvance of the ice stream (Winsborrow et al., 2010). The deglaciation in the Barents Sea show evidence of pronounced ice stream patter and dynamics (Andreassen et al., 2008, Ottesen et al., 2008), where they have been divided into three specific flow events that represent the deglaciation (Winsborrow et al., 2010). The first stage represents the Late Weichselian glacial maximum. The ice sheet covered the entire shelf and, reached the shelf edge, where the Bear Island ice stream was the main draining conduit in the area (Andreassen and Winsborrow, 2009, Winsborrow et al., 2010). The latest flow event is terminated 100 km from the shelf edge, and represent an early readvance during the deglaciation (Andreassen et al., 2008), and is suggested to have occurred at 16 000 cal. yr. BP (Winsborrow et al., 2009).

1.5.3. Holocene

The Holocene epoch, identified as the current interglacial period, began around 9.5 ka and continues to present. In the early Holocene (~9.5 – 7.5 ka), a strong input of warm and saline Atlantic water influenced the Barents Sea. This is supported by the disappearance of Arctic benthic species foraminifera in both the northern Nordic Sea and low IRD counts in the Barents Sea as well as in East Greenland and the Nordic Sea (Slubowska-Woldengen et al., 2008) as well as the distribution of dinocysts in two age-constrained sediment cores from southwestern Barents Sea (Voronina et al., 2001). Based on these reconstructions, the environment has been interpreted to have been relatively warm and stable during the early Holocene (Voronina et al., 2001). However, an "8.2 ka" cooling event lead to a short-lived cold interval (~8.2-8.1 ka BP) causing a salinity anomaly as well as a decrease in methane concentrations and the North Atlantic thermohaline circulation, resulting in an increase in sea ice (Alley et al., 1997, Alley, 2007).

The strong influence of Atlantic water weakened from 7.5 ka BP, accompanied by a north-eastward retreat of the Arctic Front (Aagaard-Sørensen et al., 2010). According to Voronina et al. (2001) the southeastern Barents Sea experienced several episodes of decreased temperatures and subsequent expansion of ice cover.

The Neoglaciation, referred to as a cold period, began around 4 ka BP and lasted to 2 ka BP (e.g. Koç et al., 1993). A climate worsening, as well as a reduced flux of Atlantic Water relative to in the early Holocene, have been documented by benthic foraminifera (Ślubowska-Woldengen et al., 2008). The shelf bottom waters experienced a cooling and freshening, whilst the sea ice cover increased. Simultaneously, iceberg rafting enhanced, possibly due to glacier re-advances on Svalbard and Greenland (e.g. Funder, 1989; Svendsen and Mangerud, 1997).

The period from 2.5 ka BP and up to present have been characterized by unstable conditions. Occurrences of reduced surface and subsurface water salinity, high IRD deposition and a stronger stratification of the water column than at present characterized the period. The southwestern Barents Sea experienced an increased influence of coastal water along with colder conditions (Risebrobakken et al., 2010).

1.6. Contourites

On the North Western Norway and South Western Barents Sea continental slope, thick packages of glacigenic debris flow interbedded with hemipelagic and contouritic sediments

compose a thick Plio-Pleistocene prograding wedge (Dahlgren et al., 2002; Hjelstuen et al., 2004). The wedge lays marginal to the former ice sheets and show evidence of active along slope following currents that have caused sediment erosion and/or deposition (Dahlgren et al., 2002; Laberg et al., 2005).

Sedimentary processes on the continental margins are related to the ability of the ocean currents to erode. These currents are driven by the interaction between the ocean and the atmosphere, and are controlled by the influence of wind currents, Coriolis effect and the shape of the ocean basins, which will determine the strength of these currents (Laberg et al., 2005).

Contourites have been deposited on the continental slope during low-stand (glacials) and high-stands (interglacials) of the sea level. Studies show that even though the currents were weaker during the glacials, the sedimentation rates on the drifts were higher, this due to the glaciomarine sediment supply from the ice sheets grounded on the continental shelf (Laberg and Vorren, 2004).

In the slides on the slope, observed evidence of mass wasting processes have affected the glacigenic debris-flow and contourites deposits. This is shown by that the glide planes of the slide are located within the contourite drift and are parallel to the original acoustic lamination. The weak layers that induced the slope failure were a depositional surface of contouritic sediment (Laberg et al., 2005)

2. Material and Methods

The sediment core investigated in this study was collected during a cruise in May 2013 with the research vessel R/V Helmer Hanssen from University of Tromsø, the Arctic University of Norway.

2.1. Sediment core

The sediment core HH13-243GC was collected from the SW Barents Sea Slope, at a water depth of 1448 m using a gravity corer. The location was decided based on the chirp data. For further details about the position and times see table 1.

The gravity corer (GC) on board of R/V Helmer Hanssen consist of a 6 m-long steel barrel with a 1600 kg weight at the top. A 6 m long plastic liner with an inner diameter of 11 cm was inserted and secured inside the steel barrel with a core cutter and a core catcher attached at the base. The gravity corer is lowered from the side of the vessel, and can by the help of the gravity from the weight on top of the device penetrate the sediments at the seafloor. The shape of the core catcher makes it easier to cut into the sediment. The core cutter encloses at the base, preventing the sediments from falling out during the transport to the surface. This is supported by a small vacuum that is produced when a valve at the top of the instrument is closed.

When the gravity corer is retrieved on board, the plastic liner is removed from the steel barrel and divided into 1 m-long sections. The sections are cleaned, labeled and secured with plastic caps at the ends. The core sections have been stored at 4°C until opening.

Tabel 1: Gravity core location and information about the core.

Station	Date	Location	Latitude[N] Longitude [E]	Water depth [m]	Recovery [cm]	Comment
HH13-243GC	27.08.2013	SW Barents Sea slope, in Bear Island Slide	71°.57.875´ 014°17.939	1448	583	6 sections

2.2.Laboratory work

The laboratory work was carried out at the Department of Geology at the University of Tromsø, The Arctic University of Norway. Radiocarbon dates were analyzed at the ^{14}Chrone Center, Queen`s University, Belfast, United Kingdom. Samples analyzed for $^{13}C/^{12}C$ and $^{18}O/^{16}O$ were sent to the Geological Mass Spectrometer Laboratory at The University of Bergen, Norway.

2.2.1. Multi Sensor Core Logger (MSCL)

Prior to opening, the core was logged with a GEOTEK Multi Sensor Core Logger (MSCL). This logging device provides continuous centimeter-scale measurements of the marine sediment core (Figure 3). The main physical properties that were measured using the MSCL were the wet bulk density, acoustic impedance, fraction porosity and magnetic susceptibility.

The cores were stored in room temperature a while before measuring, consequently to avoid disturbance of the p-wave velocity and magnetic susceptibility as they can be influenced by the temperature differences (Weber, et al., 1997; GEOTEK, 2014a). The core sections were logged continuously with a spatial interval of 1cm with a 10 seconds measuring time.

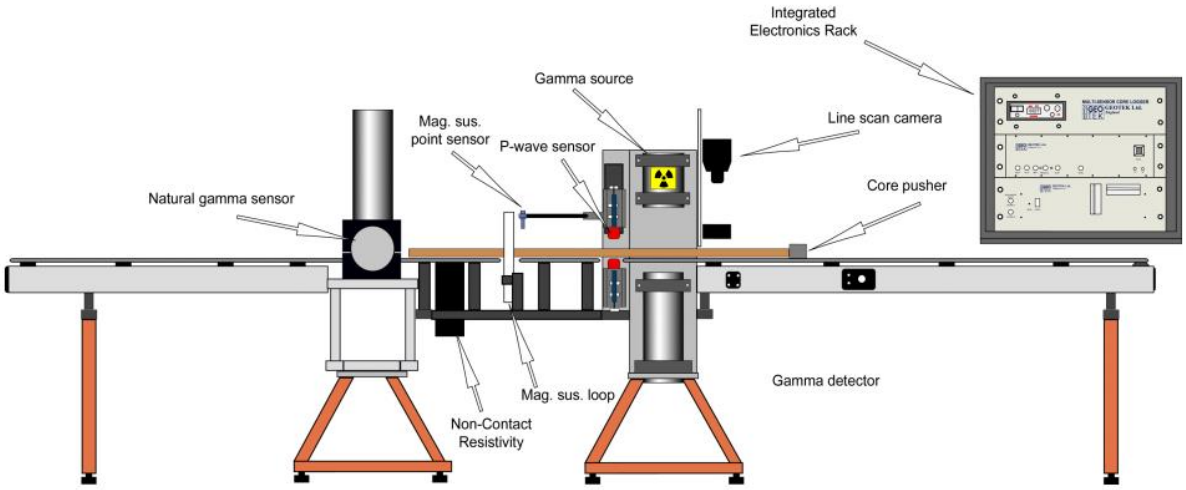

Figure 2: Principle sketch showing the setup of the Multi-Sensor Core logger (GEOTEK, 2000). The MSCL used at the Department of Geology, University of Tromsø, the Arctic University of Norway, has all instrument measuring horizontally, not vertically as in the sketch.

2.2.1.1. Wet-bulk density

The density (ρ) of a material is given by the ratio of its mass (m) to its volume (V). The bulk density is defined as the mass of any particles of the material divided by the total volume they occupy. Therefore, the sediments mineral composition and compaction will affect the bulk density (GEOTEK, 2014a).

A small beam of radioactive ^{13}C is emitting γ-ray with an energy of o.662MeV to pass through the core sections, these photons are detected on the other side and calculate the core diameter and electron density of the material. The photons that pass through the core interact with the electrons and loses energy due to Compton scattering, causing γ-ray attenuation. The measured number of photons that pass un-attenuated through the core, determines the density of the core material (GEOTEK, 2014a). Since the sediments measured in this study were wet, the obtained density is the wet bulk density (WBD).

2.2.1.2. Fraction porosity

The gamma density measurements reveal the wet-bulk density of the sediment core. From these measurements, the porosity can be calculated depending on the mineral grain density (MGD) and the fluid density (WD). The fraction porosity (FP) is then calculated by the formula:

FP = (MGD - GD1) / (MGD - WD)

Where MGD is the mineral grain density (gm/cc), GD1 is the gamma density as determined by the gamma density processing panel, and WD = fluid phase density (gm/cc) (typically 1.02) (GEOTEK, 2014a).

2.2.1.3. Magnetic susceptibility

The magnetic susceptibility (MS) is "the degree of a magnetization of a material in an applied magnetic field" (GEOTEK, 2014a). Material that are either, paramagnetic, ferromagnetic, ferrimagnetic or antiferromagnetic will all give a positive reading and strengthen the magnetic field, whereas if the material is diamagnetic the MS response will be negative and reduce the magnetic field (GEOTEK, 2014a). A magnetic field is applied to the sediment core sections as it passes through the Bartington loop sensor (MS2C) mounted on the core logger, providing down-core profiles of magnetic susceptibility at 1 cm intervals. MS data can be used to identify changes in lithology linked to shift in origin, and has been used as a stratigraphic tool to identify

events in the sedimentary record by combining and correlating several MS records with lithological analysis from the Western Svalbard Slope (Jessen et al., 2010).

2.2.2. Sedimentology

The core sections were split along the long axis with a circular saw. A spatula and a thin wire were used to cut the plastic liner and separate the sediment in the core sections in archive and working halves. The archive sections were wrapped and stored in a 4°C cooled storage room. The working section's sediment surface were cleaned and visually logged and described, taking note of the visible variations in grain size, clast distribution, sedimentary structures and contacts. Color was determined with the help of the Munsell Soil Color Chart. Lithological logs were made in Corel Draw to present the observations. By combining and using the X-radiography it is easier to identify structures, clasts and fossils which otherwise would not be easy to identify.

2.2.3. Sediment sampling

The core sections marked `Work´ was cut into 1 cm slices for the entire core length (583 samples) and put into pre-weighed and labeled plastic bags. They were all wet weighed and stored in the laboratory freezer. The sediments situated near the core liner were avoided due to possible sediment disturbance during the coring process.

2.2.4. Freeze drying

Freeze drying is done by freezing the sediments and then creating a vacuum that allows the frozen water in the sediments to sublimate from the solid phase to the gas phase. All the samples were freeze dried using the freeze dryer at the Geology Department Laboratory, UiT, Arctic University of Tromsø. This process takes approximately 24 hours, depending on the water content of the sediment samples. This process is considered to be gentler on the foraminiferal test as opposed to drying in an oven because the pore spaces are maintained after the sublimation. The water content was calculated for each sediment sample.

2.2.5. Sieving

The sample resolution for the sieving was every 10 cm the first 150 cm, and thereafter every 5cm for the rest of the core. The freeze dried samples were wet sieved in mesh sizes of 63µm, 100 µm, 500 µm and 1000 µm. Distilled water was used to get the sediment residues from the

sieving into labelled filter papers. The sieves were cleaned between each sample in a Grant XB14 ultrasonic bath and dried with compressed air to avoid contamination. The residue samples were dried in an oven (40°C) until dry. The dry samples were weighed and put into labelled glass jars.

2.2.6. Grain size distributions

The grain size distribution (>1mm; 1mm-500µm; 500µm-100 µm; 100 µm-63µm) for each sample is calculated as a percentage of the total dry weight sediment. Particle size distribution is an important diagnostic property of the sediment and may reflect changes in the sedimentary environment.

2.3. Foraminifera analysis

The 500-100 µm size fractions from core HH13-243GC were used to identify the distribution of foraminifera. This to make this study comparable to former studies from the same area, and because arctic species commonly are smaller in size compared to warmer water species.

The samples were evenly distributed on the picking tray consisting of 45 identical squares and placed under a binocular Leica CLS 150X – MZ12s microscope for analysis. Every 10^{th} sample was investigated which make up a total of 59 samples where both planktonic and benthic foraminifera were counted. Every foraminifera in random squares were counted, approximately 250 individual planktonic foraminifera were identified to species level. Over 300 individual benthic foraminifera from the same squares were counted and identified. When the number was obtained, the current square was completed. This is for a reliable statistically comparability for one population and between the samples (Phleger, 1960; Murray, 1973; Lowe and Walker, 1997). Between each sample, the equipment was substantial cleaned with compressed air to avoid and minimize contamination.

Some of the samples were relatively large, so the amount of material on the tray were weighed for later analysis and calculations of the number of foraminifera per gram (the density) and flux of foraminifera (see age model and accumulation ratio). If there weren't enough specimens in a sample, more than one tray was counted to identify a sufficient amount of specimens.

The concentrations of planktic and benthic foraminifera were calculated as number of foraminifera per gram dry weight sediment (no. foraminifera/gram):

Concentration of foraminifera (no. foraminifera/gram) = (((No. counted foraminifera/No. counted squares)*45)/weight rest. on tray*weight 500-100µm)/total dry weight

The foraminifera were all identified to species level and the percentage for each species were calculated relative to total amount of foraminifera in a sample. Some species were grouped as other/indeterminate as there was a lack of features making them hard to identify.

2.4. Color images

The scanning images of the cores were taken by using Jai L-107CC 3 CCd RBG Line Scan Camera, which is installed on the Avaatech XRF core scanner. Prior to the scanning images, the archive core sections of core HH13-243GC, were cleaned and smoothed with a plastic card.

2.5. X-ray photography

By using the x-ray photography, it is easier to detect structures, clast and fossils, which are difficult to identify by visual description.

2.6. Radiocarbon dating

2.6.1. Principle

Radiocarbon dating is widely used to determine the ages of materials younger than 50 000 years by measuring the decay of ^{14}C. Carbon has three natural occurring isotopes; atoms of the same atomic number but different atomic weights. The three isotopes ^{12}C, ^{13}C and ^{14}C do not occur equally in the atmosphere, and unlike ^{12}C and ^{13}C are ^{14}C unstable and therefore radioactive (Bowman, 1990). Carbon-14 is continually produced in the upper atmosphere by nuclear reactions between free neutrons colliding with other atoms and molecules, basically between ^{14}N atoms. The isotope is rapidly oxidized to CO_2 molecules, which is further mixed through the atmosphere and absorbed by the oceans where they enter plant material by the photosynthesis and become a part of calcareous ($CaCO_3$) marine organisms through the carbon cycle. As long as the organism is alive, it will be in equilibrium with the atmosphere, after their death the absorption of atmospheric CO_2 ends and the ^{14}C will continue to decay, but not be replaced (Lowe and Walker, 2015). The isotope has a half-life of 5570 ± 30 years, whereas the death can be calculated from measuring the number of unstable ^{14}C relative to the stable ^{12}C and ^{13}C by comparing this ratio whit that of a standard known ^{14}C content (Godwin, 1962;

Bowman, 1990; Lowe and Walker, 2015). This method is based on several assumptions. 1) The ^{14}C production in the atmosphere has been constant over time. 2) The concentration of ^{14}C is equal for all parts of the system. 3) The half-life of ^{14}C is known to an accurate and acceptable level of precision and has existed as a close system since the death of the organism (Bowman, 1990). All of these assumptions have to be taking into account as they also are sources of error when interpreting the ^{14}C ages (Faure and Mensing, 2005).

2.6.2. AMS radiocarbon dating

Radiocarbon dating was performed on five samples containing *Neogloboquadrina pachyderma sinistral (s)* at different intervals representing a wide age distribution in the core. The intervals were selected mainly where there was observed a faunal change and where there also was sufficient amount of the dating material. Only well preserved specimens of N. pachyderma (s) with no signs of damage were collected, this to avoid samples with contamination from re-deposition. The samples from core HH13-243 GC were sent to the 14CHRONO Centre at Queens University in Belfast, United Kingdom, for AMS ^{14}C dating (Table 2)

Tabel 2: Overview and information about the prepared AMS ^{14}C samples from core HH13-243 GC.

Lab reference	Core	Sampling depth (cm)	Species	Weigth (mg)
UBA-32668	HH13-243GC	80-81	N. pachy s	8.80
UBA-32669	HH13-243GC	230-231	N. pachy s	8.40
UBA-32670	HH13-243GC	320-321	N. pachy s	11.30
UBA-32671	HH13-243GC	440-441	N. pachy s	9.10
UBA-32672	HH13-243GC	540-541	N. pachy s	12.70

The principle of accelerator mass spectrometry is based on how to identify the atoms in elements based on their different atomic weights (Lowe and Walker, 2015). By accelerating C-ions from the sample that is being dated and subjecting them to a magnetic field, particles with

the same velocity, but different mass, will deflect differently towards the applied magnetic field. The heaviest particles will deflect the least, but because ^{14}C and ^{14}N have a similar atomic weight, their particles must travel at high speeds from large charge differences to distinguish between the two isotopes (Lowe and Walker, 2015), making it possible to identify and measure the amount of 14C present in the sample (Bowman, 1990; Higham et al.,2014).

2.6.3. Calibration and marine reservoir effects

The CALIB 7.1.0 program (Stuvier and Reimer, 1993) was used to calibrate the radiocarbon ages obtained from the AMS dating. The program converted all dates into calendar year's (cal. yr. BP) using the calibration curve dataset. The dataset was set to MARINE13 (Reimer, et al., 2013), with a global reservoir correction of 405 years, adjusting for the differences between ^{14}C- dated terrestrial material and marine material and is recommended for most marine samples. The marine reservoir age (ΔR) was set to be 0, due to core HH13-243GC being collected from the deep sea. The σ2 dating uncertainty was used, where the mean calibrated age was calculated and presented as calibrated calendar years before present (cal. yr. BP).

2.6.4. Age model and accumulation rates

The obtained radiocarbon dates were used for estimating an age model for the sediment core. By using a linear interpolation and assuming that the sediment rate was constant between the calendar ages derived from the ^{14} C dated samples, the linear sedimentation rate (cm ky^{-1}) was calculated, this is further described in the results. Uncertainties are to be expected, especially when there are only a few dates available.

The mass accumulation rate (MAR) is expressed as g cm^2 ky^{-1} and is calculated from the dry bulk density (DBD) to calculate the flux of the IRD and planktonic and benthic foraminifera as no. /cm^2 ky^{-1}. The dry bulk density is calculated out of the formula:

Dry bulk density = wet bulk density – (core diameter (1.026)*Porosity/100))

where MAR is the linear sedimentation rate (cm/1000yr.)*dry bulk density.
Planktic and benthic foraminiferal fluxes (no. /cm^2 ky^{-1}) were calculated using the formula:

Flux = Concentration of foraminifera (no. /gram) * Mass accumulation rate (MAR)

2.7. Stable oxygen and carbon isotope analysis

2.7.1. Principle

Stable isotope analyses of the carbon tests calcified by foraminifera have provided much of the understanding and foundation of reconstructions of past ocean and climate conditions (Katz et al., 2010). Variations in the ratios between the isotopes of carbon and oxygen ($\delta^{18}O$, $\delta^{13}C$) in the foraminiferal tests reveal several geochemical properties of the ambient sea water masses in which they have been calcified. More specifically, $\delta^{18}O$ is controlled by temperature and salinity changes, whereas $\delta^{13}C$ reflect the primary production and stratification characteristics of the water mass (e.g. Spielhagen and Erlenkeuser, 1994; Katz et al. 2010; Berben, 2014), and therefore provide a basis for the reconstruction of oceanographically changes (Lowe and Walker, 2005). Planktic foraminifera provide information of the surface ocean, whereas benthic foraminifera provide information on conditions at the seafloor and in shallow pore waters, from shallow seas to deep ocean basins (Katz et al. 2010; Berben, 2014).

2.7.2. Oxygen isotope

Oxygen can exist in three isotopic forms ^{16}O, ^{17}O and ^{18}O, but only ^{16}O and ^{18}O are of more importance in oxygen isotope analysis of marine deposits. The ratios between $^{16}O/^{18}O$ in the natural environment is approximately 1:500. The ratios of the isotopes are not measured accuracy but as relative deviations from a laboratory standard.

Oxygen isotope ratios are then expressed as positive or negative values relative to the standard ($\delta = 0$), thus:

$$\delta^{18}O = 1000 \text{ x } \frac{18O/16Osample - 18O/16Ostandard}{18O/16Ostandard}$$

The changes in the values measured in the marine microfossils are a result of fractionation of oxygen isotopes as water evaporates from the surface (Lowe and Walker, 2015). The isotopes have different masses, which will affect the mass of the element they bond with, like H_2O (Faure and Mensing, 2005). Water molecules consist of either the heavy or the light isotope, so during the evaporation, the lighter $H_2{}^{16}O$ molecule is drawn into the atmosphere in preference to the heavier $H_2{}^{18}O$ molecule. Since this process is temperature dependent, it will in higher latitudes where colder air masses are increasingly less able to absorb the heavier isotope produce ^{16}O-enriched precipitation. The precipitation will in glacial periods be stored/trapped in ice and cause the glacial ice to be enriched with ^{16}O- molecules, while the oceans is rich in the heavier

^{18}O- molecule (i.e. isotopically more positive, or heavier)(Katz et al., 2010; Lowe and Walker, 2015). However, during interglacial periods the melting of ice will move large volumes of water enriched in ^{16}O- molecules back into the oceans. This results in oscillation in the marine oxygen isotope signal display glacial and interglacial conditions (Lowe and Walker, 2015). The $^{16}O/^{18}O$ ratio in foraminifera reveals that the overall glacial/interglacial variation is small, and regardless whether the benthic species have much heavier $\delta^{18}O$ values than surface species, they match very closely. This suggests that in spite of the influence of other factors, they show good indicators of global ice-storage signal (Lowe and Walker, 2015).

The foraminifera tests, which is made up of calcium carbonate, record the ambient seawater (δw), and will therefor reflect (1) the global ice volume and (2) region/local river-water input (3) evaporation/precipitation for shelf and surface waters (Katz, et al., 2010).

The oxygen isotope analysis has some limitations:

Biological vital effects could cause some species to calcify in disequilibrium with the seawater. Some species are therefore to prefer as they are known to calcify in equilibrium, such as *Uvigerina senticosa* and *Globocassidulina subglobosa.* Some planktic species also calcify at different depths in their lifecycle, witch lead to differences in isotopic ratios between adults and juveniles. Sediment mixing caused by bioturbation or other processes such as turbidity current and bottom dwelling could affect the isotope record by reworking of the sediments.

2.7.3. Carbon isotope

Carbon has two natural occurring stable isotopes; ^{13}C and ^{12}C, they are because of oxidization incorporated into carbon dioxide (CO_2), and fractionations of carbon occurs during various natural processes (chemical and biological)(Lowe and Walker, 2015). The carbon isotopic ratio $^{13}C/^{12}C$ is expressed as $\delta^{13}C$, and is a function of temperature and isotopic composition of the dissolved inorganic carbon (DIC) in seawater. Carbon isotope ratios are then expressed as positive or negative values relative to the standard (δ = 0), thus:

$$\delta\,^{13}O = 1000 \text{ x } \frac{13C/12Csample - 13C/12Cstandard}{13C/12Cstandard}$$

The terms enriched/depleted, heavier/lighter and positive/negative is referring to the increase or decrease of the heavy isotope ^{13}C (Armstrong and Braiser, 2005). The isotopic record of

carbon can be used in reconstructions of ocean circulation, marine productivity, air-sea gas exchange, and biosphere carbon storage (Oliver et al., 2009). As with oxygen isotopes, the carbon isotopes have different masses, making one of them in favor in the fractionation process. Photosynthesis is the dominating fractionation method, and ^{12}C is biologically preferentially absorbed during photosynthesis due to it is isotopically lighter, leading the earth`s biosphere with negative $\delta^{13}C$ (Katz et al., 2010).

The $\delta^{13}C$-values in the upper water masses tends to be greatest during glacial periods and least during interglacial periods (Armstrong & Braiser, 2005), whereas the $^{13}C/^{12}C$ ratio in dissolved carbon in the deep ocean is lower during glaciations (Shackelton, 1977).

Ventilation of deeper water masses trough vertical circulation brings oxygenated water into deeper parts of the ocean. With reduced vertical mixing, oxygen level falls and the productivity is reduced, reflecting $\delta^{13}C$ signal. Deep water masses have marked $\delta^{13}C$ characteristics and measurements from benthic foraminifera, resulting in information about the bottom circulations and ventilation changes in the oceans (Lowe and Walker, 2015).

2.7.3.1. Paleoproductivity

Studies show that organic matter from the surface ocean is the primary food supply for benthic foraminifera, and hence the surface water productivity is a primary control on the species composition, accumulation rate, and geographic distribution of benthic foraminiferal faunas (Katz et al., 2010). Since the phytoplankton preferentially take up ^{12}C during photosynthesis, ^{12}C-enriched organic matter sinks from the surface water to the sea floor, leaving the surrounding surface waters enriched in ^{13}C giving higher $\delta^{13}C$ values, and lower $\delta^{13}C$ values at the sea floor as oxidation of organic matter releases nutrients and $^{12}CO_2$. High export production will therefore drive $\delta^{13}C$ higher in planktic and lower in benthic foraminifera, resulting in an offset between the two. For instance, a decrease in planktic foraminiferal flux and simultaneously an increase in benthic flux may indicate higher surface ocean primary productivity, which will be explained by higher food supply to the benthic community. Comparisons with epifaunal and infaunal benthic foraminiferal $\delta^{13}C$ may reflect the presence and preservation of organic matter and ventilation (Katz et al., 2012).

2.7.4. Stable isotope analysis

The isotopic measurements were carried out using a FInnigan MAT 253 spectrometer with a Kiel IV device at the Geological Mass Spectrometer (GMS) laboratory at the University in Bergen. Stable isotope ($\delta^{18}O$, $\delta^{13}C$) analyses were performed on the foraminiferal test of N. pachyderma (s), Cassidulina neoteretis, *Cibicidoides wullestrofi* and *Cibicidoides lobatulus*. All specimens were selected from a size range between 500-100µm and species with no damage and approximately the same size were gathered, this in order to minimize size dependent effects on isotopic composition (Bauch et al., 2000). The foraminifera were all picked based on their preservation state and where possible. Sufficient specimens were obtained from 58 samples of N. pachyderma (s), 49 samples of C. neoteretis, 17 samples of C. *wullestrofi* and 18 samples of C. *lobatulus* using a binocular microscope (Leica CLS150X – MZ12s). Samples were crushed and cleaned with methanol in an ultrasonic bath before being measured. The precision for $\delta^{18}O$ was ±0.06‰ and ±0.03‰ for δ13C versus the PeeDee Beleminite after calibration with the standard. All values are presented as per mill (‰).

The infaunal foraminifera *Cassidulina neoteretis* where selected due to it being continuously present in the core and a suitable proxy for pore water conditions. While C. lobatulus and C. wullestrofi are one of the most used epifaunal species (Katz et al., 2010), they are selected for an overlap for reconstructions of the bottom water ventilations as they each are represented in the different half of the sediment core (see results in chapter 5). While the high amount of N. pachyderma will give a continuously record of the surface water conditions.

As some species do not calcify in equilibrium with the ambient seawater, $\delta^{18}O$ values for some species must be corrected for vital effects. C. lobatulus and C. wullestrofi where both corrected for +0,64 ‰ (Shackleton, 1974). There is some disagreement whether C. neoteretis needs some correction, however, in this study and some other studies in the same area, no correction was facilitated due to that it is considered to be in equilibrium with the ambient water (Duplessy et al., 1980; Poole, 1994). To correct for the ice volume changes in oxygen isotopes, the sea-level curve from Grant et al. (2014) was used. Global ice volume causes 0.11‰ changes in the δ18O every 10 meters of sea level change.

3. Foraminifera

3.1. Introduction

Foraminifera are single celled organisms that today can be found in environments ranging from deep-sea to inner fjords. They are abundant on continental shelves and slopes, and respond to various environmental settings. Planktonic foraminifera live in the water masses at various depths, while benthic species live near, on or in the sediment (Tosk, 1988). The foraminifera consist of a soft body enclosed within a shell or "test" secreted by the organism, which is variously composed of minerals (calcite or aragonite), organic matter (tecthin) or agglutinated components (Lowe and Walker, 2015). When the foraminifera form their test, they precipitate different chemical components from the seawater, which reflects the properties of the seawater at that time of formation (Katz et al., 2010). When they die they sink to the seafloor and get incorporated into the sediments and are then a part of the marine sedimentary archives (Rasmussen and Thomsen, 2015).

The study of the relationship between the environment and living organism is termed ecology (Armstrong and Braiser, 2005), the study and the understanding of modern and ancient marine environment have proven to be important in terms of paleo-reconstructions (Corliss, 1985). The distribution of the foraminifera assemblage are influenced by different ecological factors such as; salinity, temperature, oxygen, currents and turbidity, light and organic and nutrient flux within the water column (Armstrong and Braiser, 2005; Murray, 2006).

Because they are known to inhibit most of the marine habitats and have strong environmental preference (Hald and Steinsund, 1992; Corliss and Shiva, 1993; Hunt and Corliss, 1993; Hald and Korsund 1997; Korsun and Hald, 1998; Wollenburg and Mackensen, 1998, Polyak et al., 2002; Zajaczkowski et al., 2010), they are used as reliable proxy for paleoceanographic and paleoenvironmental reconstructions.

The distribution of modern planktic and benthic foraminifera assemblage living in various environmental conditions in the South Western Barents Sea, the Nordic seas and the Arctic have provided an important analogue that can be applied to the interpretation of paleoenvironmental and paleoceanographic reconstructions of the Quaternary (Sejrup et al., 2004;Saher et al., 2012). There are several studies from the slope and shelf along the continental margin in the Nordic and Barents seas based on the comparison of the fossil foraminiferal

record with the modern distribution (e.g. Hald and Steinsund, 1992; Hald and Aspeli, 1997; Bauch et al., 2001; Rasmussen et al., 2007; Slubowska-Woldengen et al., 2008).

3.2. Fauna modification

The proportion of calcareous foraminifera tends to decline with increasing water depth (Douglas, 1981; Hughes et al., 2000) due to carbonate dissolution (Berger, 1979), and below the Carbon Compensation Depth (CCD; below > 4000m) there are no or little calcareous species to be found (Lowe and Walker, 2015). However, other processes can influence the fauna composition and distribution. High content of organic material on the sea floor causes bad preservation and carbonate dissolution due to increase of oxidation and further increase of CO_2 (acidic water). Redistribution due to secondary processes can modify the sediments and lead to misinterpretations of the data (Steinsund et al., 1994). Re-sedimentation, bioturbation and diagenesis can all contribute to modifications; yet, the foraminifera in core HH13-243GC show little signs of diagenesis or abnormal corroded calcareous foraminifera. Eventual signs of re-sedimentation and bioturbation will be discussed in chapter 6.

3.3. Planktonic foraminifera ecology

Planktonic foraminifera are one of the most common groups of pelagic organisms in the open ocean (Be´ and Tollerlund, 1971). They are the major contributors to deep-sea sediments with some other calcareous species, which account for more than 80 per cent of modern carbonate deposition in the oceans (Hüneke and Mulder, 2011). They thrive in the open ocean and usually avoid coastal areas, shallow shelf and fjords, but can come close to land with steep shelf areas (Lowe and Walker, 2015). The planktic foraminifera fauna reflects the sea surface conditions and have rather specific environmental preferences. Their distribution and restrictions of the various species groups are today imposed by their dependence on particular water masses (Be´ and Tollerlund, 1971) with narrow temperature range (Pflaumann et al., 2003) where the controlling factors are the temperature, salinity, nutrition and sea-ice cover (Berben, 2014).

The main species of planktic foraminifera in HH13-243GC are the *Neogloboquadrina pachyderma (s), Turborotalita quinqueloba, Neogloboquadrina pachyderma (d) and sporadic occurrences of Globigerina bulloides, Globigerinata glutinata* and *Globigerinita uvula* witch will just be describe briefly.

3.3.1. Dominating species

3.3.1.1. Neogloboquadrina pachyderma (sinistral) (Ehrenberg,1861)

The *Neogloboquadrina pachyderma (sinistral),* herafter *N.pachyderma (s)* is the most abundant planktic species in core HH13-243GC. This polar species is a cold-water indicator which is dominant in the Antarctic and Arctic seas, as well as in the Arctic and Polar Water in the North Atlantic (Be´and Tollerlund, 1971; Johannesen et al., 1994; Pflaumann et al., 2003). This species makes an important proxy for determining temperature, salinity, sea ice and nutrient conditions in the past and often reflect polar surface water and glacial conditions (Bauch et al., 2001). *N. pachyderma (s)* thrives in deeper water masses at 25-250 m below the thermocline (Stmstich et al., 2003) and is dominant in samples north of the Arctic Front in the Greenland, Iceland and Norwegian Seas (Johannesen et al., 1994; Pflaumann et al., 1996; Kohfeld et al., 1996). The N. pachyderma (s) prefer sea surface temperature (SST) <5°C and during summer <8°C (Pflaumann et al., 1996). In shorter timescales, abundance changes in *N. pachyderma (s)* have been interpreted by Broecker et al. (1990) to reflect temperature changes during rapid climate change events in the North Atlantic, such as the Younger Dryas (Kohfeld et al., 1996). They also records changes in the North Atlantic surface ocean and are in conjunction with the atmosphere based on the $\delta^{18}O$ in *N. pachyderma (s)* and the Greenland ice cores (Kohfeld et al., 1996).

3.3.1.2. Neogloboquadrina pachyderma (dextral) (Ehrenberg, 1861)

Neogloboquadrina pachyderma (dextral), hereafter called *N. pachyderma (d),* is a planktonic foraminifera that resembles the *N. pachyderma (s)* but the test coils in the opposite direction (dextral). Also, the foraminifera has the opposite preference of water temperature and is considered to be a warm water indicator of the Norwegian-Barents Svalbard margin (Hald et al., 2007) preferring a temperature around 12°C (Schmidt et al., 2004). Its maximum distribution is linked to the influx of Atlantic Water in the northern North Atlantic (Be´and Tolderlund, 1971; Johannessen et al., 1994). Darling et al. (2006) propose that *N. pachyderma (d)* should be called *N.incompa* and be considered as a different species based on the coiling direction and water preferences.

3.3.1.3. Turborotalita quinqueloba (Natland, 1938)

Turborotalita quinqueloba is a subpolar species (Bauch, 1994), and is one of the most important species living in Atlantic surface waters at high northern latitude (Be`and Tolderlund, 1971), associated with the oceanic fronts (Johannessen et al., 1994). T.quinqueloba indicates the advance of the Arctic Front (dividing the Arctic and Atlantic Waters), or the Polar front (dividing Polar and Arctic Waters) (Johannesen et al., 1994; Pflaumann et al., 2003), where nutrient content is high (Carstens et al., 1997). This species is a surface dweller occurring at 25-75m (Simstich et al., 2003) and responds rapidly to changes in nutrient supply (Reynolds and Thunell, 1985). This species is the most abundant and widespread of all subpolar foraminifera. In the Nordic seas, T. quinqueloba is most abundant in Arctic surface water and cooler Atlantic surface water (Be´and Tolderlund, 1971; Johannessen et al., 1994; Rasmussen and Thomsen, 2010). The species often reflect the oceanographic changes that arise after pronounced glacial periods where the inflow of Atlantic Water affects the water circulation in the area (Bauch 1994; Hebbeln et al., 1994).

3.3.2. Sub-dominating planktic species

3.3.2.1. Globigerina bulloides d´Orbigny, 1826

Globigerina bulloides is a subpolar species, associated with inflow of warm Atlantic surface water (Rasmussen et al., 2007). The species is today most abundant in the northernmost Atlantic linked to the relatively temperate Atlantic waters of the Irminger Current southeast of Iceland where it reaches up to 60% of the total fauna (Pflaumann et al., 2003). *G. bulloides* is not found in large quantities on the continental margin off northern Norway, Barents Sea and Svalbard, but had its maximum abundance during the early Holocene and when the surface waters is between 11-16 °C (Be´and Tolderlund, 1971; Hald et al., 2007).

3.3.2.2. Globigerinita glutinata (Egger, 1893)

Globigerinita glutinata is a subpolar cosmopolitan species, it is recorded in a wide temperature range from 2,5°C to 29,5°C and over nearly the entire range of average surface salinity (e.g. Tolderlund and Be´, 1971).

3.3.2.3. Globigerinita uvula (Ehrenberg, 1861)

Globigerinita uvula is an opportunist species, which is most abundant in the South Atlantic but is also found in upwelling areas affected by the Polar front. The species likes cold productive surface waters (Boltovskoy et al., 1996; Rasmussen et al., 2007). *G. uvula* has a wide sea surface temperature (SST) range of ~3- > 15 °C (Rasmussen and Thomsen, 2008).

3.4. Benthic foraminiferal ecology

Water depth was once thought to be the primary factor controlling the distribution of benthic foraminifera (Mackensen et al., 1985). In recent studies, however, the distribution of deep-sea benthic foraminifera is controlled by the availability of food and competition between the species, while hydrography of different water masses and their characteristics are considered to be of lesser importance (Wollenburg and Mackensen, 1998). The benthic foraminifera are classified according to their preferred microhabitat, either infaunal or epifaunal. Infaunal species live within the top 200-10 mm and epifaunal are most free living on the seafloor but can also be found attached to the substrate or to the shell of another animal (Mackensen et al., 1985). Because infaunal species depend on the availability of food and/or reduced pore water oxygen contents, high infaunal activities are usually correlated with reduced current activity so there is an accumulation of food supply (Wollenburg and Mackensen, 1998). Epifaunal species, nonetheless, dominate when oligotrophic conditions triumph, and can therefore be an indicator of paleo-productivity in the area (Katz et al., 2010).

The agglutinated species are absent except for a few single specimens of *Cribrostomoides subglobsum* (Cushman, 1910), which is present in the top cm of the core. However they will not be discussed further and are excluded from the diversity estimates.

3.4.1. Dominating species

3.4.1.1. 'Atlantic species group'

This species group consists of various benthic foraminifera that can be found in in high abundance at intermediate depths in the Atlantic Ocean (Phleger et al., 1953). They are today most abundant in the Mediterranean Sea, on the west European Seaboard, in the Gulf of Mexico, and in the southern Labrador Sea at mid-depth (Rasmussen and Thomsen, 2004), connected to relatively warm waters (Rasmussen et al., 1996a,b). They do not occur in the Nordic Seas today

(Rasmussen et al., 1996 a,b; Wullenburg et al., 2004). The group thrives and is commonly found in temperatures >3,5°C and has not been reported from areas below 2°C (Rasmussen et al., 1996b).

Studies indicate that this group are occurs where there is bottom water warming due to prevented heat loss caused by meltwater and sea ice cover (Duplessy et al., 1975; Rasmussen et al., 1996a; Rasmussen and Thomsen, 2004; Wullenburg et al., 2004).

The 'Atlantic species group' consist of: *Sigmoolopsis schlumbergeri* (Silvestri, 1904), *Eggerella bradyi* (Cushman,1911), *Bulimina costata*; d´Orbigny, 1852, *Anomalinoides minima* (Forster, 1892), *Gyroidinoides umbonata* (Silvestri, 1898), *Eilohedra nipponica (*Kuwano, 1962*)*, *Cibicides pachyderma* (Rzehak, 1886), *Pygro Williamsoni* (Silvestri, 1923) and *Valvulinera arctica*; Green 1959.

3.4.1.2. Cassidulina neoteretis Sidenkrantz, 1995

Cassidulina neoteretis is an infaunal species (Mackensen and Hald, 1988) that prefers chilled Atlantic Water (- 1 to + 2 °C) overlain by cold-water masses (Jennings et al., 2004) and saline (34.9‰) bottom water conditions (Jansen et al., 1990). C. neoteretis inhabits shallow shelf to deep-sea environments (150-3000m) (Steinsund et al., 1994; Mackensen, 1998), and is typically abundant in fine-grained organic rich muds and glaciomarine settings (Mackensen and Hald, 1988; Seidenkrantz, 1995). This species is often found together with high concentrations of planktonic foraminifera and is suggested to be typical of seasonally ice-free conditions (Polyak and Mikhailov, 1996; Slubowska-Woldengen et al., 2008). This is an important species in the Barents Sea north of 72 °N (Mackensen and Hald, 1988).

3.4.1.3. Cassidulina reniforme Nørvang, 1945

Cassudulina reniforme is an infaunal species that lives in within the 5 topmost centimetres of the sediments on the sea floor (Hald et al., 1997). This is an opportunist Arctic-Polar species that thrives in cooled Atlantic Water (Hald and Korsund, 1997) and tolerates relatively low salinity (>30‰) and temperatures down to the freezing point (Steinsund et al., 1994; Hald and Steinsund, 1996), with seasonal sea ice coverage (Polyak et al., 2002). *Cassidulina reniforme* prefers muddy sediments at deeper depths and low turbidity (Steinsund et al., 1994), occurring frequently in distal glaciomarine environments (Sejrup et al., 1981; Rasmussen et al., 2007).

Due to its small size, they are often considered to be reworked, subjected to redisposition by down-slope gravity flows (Mudie et al., 1984).

3.4.1.4. Cibicides lobatulus (Walker and Jacob, 1798)

Cibicides lobatulus is considered to be an epifaunal species that thrives on coarse substrates under strong currents conditions (Jennings et al., 2004). The species is primary an indicator of high energy environment with low sedimentation rates as the strong currents prevent sedimentation of fine grained material (Klitgaard Kristensen and Sejrup, 1996; Hald and Korsund, 1997) and high food supply (Hald and Steinsund, 1992). *C. lobatulus* covers a wide temperature range, but prefer normal salinity >32‰ (Steinsund et al., 1994), associated with warm saline Atlantic water (Mackensen et al., 1985).

3.4.1.5. Cibicides wuellerstorfi (Schwager, 1866)

Cibicides wuellerstorfi is a deep-water species that indicate interglacial water-mass conditions in the Nordic seas (Bauch et al., 2001). The specie is an epifaunal suspension feeder and an indicator of bottom current activity and is in the Norwegian Sea related to increased nutrient supply (Mackensen, 1985). This all fits with the interglacial appearance of *C. wuellerstorfi* where it may be a benthic response to changes in the surface water conditions (Hald and Aspeli, 1997). *C. wuellerstorfi* is often found together with *Epistominella exigua* (Brady, 1884) (another deep-water species) in sediment samples containing high amount of sand (Mackensen, 1985). *C. wuellerstorfi* often correlates with high seasonal primary production (Sun et al., 2006).

3.4.1.6. Elphidium excavatum forma clavata (Cushman, 1939)

Elphidium excavatum forma *clavata*, herafter *E. excavatum*, is a deep infaunal species. Its distribution in the Barents Sea is according to Steinsund et al. (1994) exclusively confined to the Arctic waters with winter sea ice cover. *E. excavatum* is associated with high turbidity waters, high sedimentation rates and to ice-proximal environments (Hald et al., 1997). It is an opportunistic species and is well adapted to tolerate fluctuating environmental conditions (Hald et al., 1994). This is often an unfavourable environment for other species and why this species is observed in low diversity faunas as it uses this environment to its advantage (Polyak et al.,

2002). *E. excavatum* prefer shallow waters were the temperatures is below 1 °C and where the salinities is between 30-34‰ (Steinsund et al., 1994; Hald and Korsund 1997).

3.4.1.7. Islandiella helenae and norcrossi Feyling-Hanssen & Buzas, 1976; (Cushman, 1933)

These two species are relatively similar in appearance, and will mainly consist of *Islandiella norcrossi* with a few *Islandiella helenae.* They are grouped together and will be represented as *Islandiella norcrossi* hereafter.

Islandiella norcrossi is an Arctic-Polar epifaunal/ shallow infaunal species (Steinsund et al., 1994; Slubowska-Woldegen et al., 2008). They are in the Barents Sea found in association with seasonal sea ice, where it is in high concentration during ice melting using the edge-algal blooms as a food source (Steinsund et al., 1994; Polyak et la., 2002). *Islandiella norcrossi* prefers relatively stable bottom waters salinities (Korsund and Hald, 1998). The species are dominating in the Norwegian – Greenland Seas from 660-1200 meters (Belanger and Streeter, 1980), and are in the modern environment abundant in distal glaciomarine sediments with ice rafted debris and marine mud (Korsund and Hald, 1998).

3.4.1.8. Melonis barleeanus (Williamson, 1885)

Melonis barleeanus is an infaunal species (Jennings et al., 2004) associated in areas of episodic primary productivity, often related with the flow of chilled Atlantic-delivered waters. In the Barents Sea it is confined to areas with normal salinities higher than 32‰ and to water flows with temperatures between 3-4°C (Steinsund et al., 1994). *M. barleeanus* is adapted to feed on partially degraded organic matter buried in preferable muddy sediments in the south western Barents Sea (Hald and Steinsund, 1992; Jennings et al., 2004), and can change between infaunal and epifaunal habitat depending on food supply and environmental conditions (Linke and Lutze, 1993).

3.4.1.9. Nonionellina labradorica (Dawson, 1860)

Nonionellina labradorica is an Arctic-Polar species known to be a deep infaunal dweller feeding on buried organic matter (Corliss, 1991; Steinsund et al., 1994). *N. labradorica* prefers cold water (<2°C) with salinities around 33-34 ‰ and is abundant in areas with high organic matter, like on the slopes of banks. This species can be found in high concentrations along

oceanic fronts and where seasonal productivities are high at ice-marginal zones (Steinsund et al., 1994). Today, the *N. labradorica* is found in the outer fjords of Svalbard in distal glaciomarine environments in association with Atlantic Water (Hald et al., 1997).

3.4.1.10. Oridorsalis umbonatus (Reuss, 1851)

Oridorsalis umbonatus is a shallow infaunal species that occupies the uppermost centimetre of the sediments (Rathburn and Corliss, 1994; Bauch et al., 2001). The species usually represent interglacial conditions and are in the Nordic seas found in deep food starved basins (Mackensen et al., 1985; Rasmussen et al., 2007). In the deep sea *O. umbonatus* is often accompanied by *Trifarina frigda*, where they both prefer a relatively high oxygen content in the sediments, but tolerate as mentioned relatively low food supply (Mackensen et al., 1985). This correlates well with recent studies, showing that *O. umbonatus* dominate periods with more ice-covered sea surface (Streeter et al., 1982; Jansen et al., 1983).

3.4.2. Sub-dominating benthic species

3.4.2.1. Astrononion gallowayi Loeblich & Tappan, 1953

This species is often found together with C. lobatulus, which is indicative of high-energy environments (Polyak et al., 2002). *Astrononion gallowayi* is related to coarser sediments (Jennings et al., 2004) and is observed on the shelf and upper slope of the Barents Sea in conjunction with epifaunal life mode of this species (Korsund and Polyak, 1989; Wollenburg and Mackensen, 1998; Polyak et al., 2002). It thrives in environments with low temperature <1°C and salinities around >30‰ but prefers >33‰ (Steinsund et al., 1994).

3.4.2.2. Buccella spp (Cushman, 1922; Bandy, 1959)

This group consist mainly of *Buccella frigida* and a smaller portion of *Buccella tenerrima*, hereafter called *Bucccella spp*. They have similar morphology and environment preferences.

They are either epifaunal or shallow infaunal species (Rosoff et al., 1992) that are most abundant in areas with frequent sea ice formation, primary linked to high seasonal productivity (Steinsund, 1994; Polyak et al., 2002). Studies from the Barents Sea show that they prefer water depths of 100-200m, low temperatures 0-1°C and salinities around 33-34‰ (Steinsund et al.,

1994), but can tolerate a broader spectre (Hald and Steinsund, 1996). *Buccella spp* is typicaly found together with *Islandiella norcrossi/helenae*, in areas of seasonal sea-ice cover, where ice-edge productivity blooms occur during spring/summer season (Steinsund et al., 1994).

3.4.2.3. Cassidulina leavingata d´Orbigny, 1826

Cassidulina leavingata is in the North Sea and in the Barents Sea recorded in connection to the warm Atlantic Water (e.g. Mackensen et al., 1985). This boreal species is in the Barents Sea excluded to habitat areas with bottom water temperatures over 2°C (Mackensen and Hald, 1988).

3.4.2.4. Cassidulina obtusa Williamson, 1858

Cassidulina obtusa is a boreal species that occur together with similar species that thrives in boreal environment. The specie has a similar appearance as *Cassidulina reniforme*, however, it prefers as mentioned an arctic environment. Therefore, it is important to distinguish these species when interpreting fossil faunas (Sejrup and Guilbault, 1980).

3.4.2.5. Epistominella exigua and Ioanella tumidula (Brady, 1884)

They are both opportunistic species, which correlates with pulses of nutrient supply and seasonal primary production (Gooday, 2003). Today they are found on the slope of western Barents Sea at a depth around 1200 meters (Rasmussen et al., 2007), and are largely controlled by the presence of organic material on the seafloor (Sun et al., 2006).

3.4.2.6. Stainforthia loeblichi Feyling-Hanssen, 1954

Stainforthia loeblichi is an opportunist species with a patchy distribution, with maximum concentrations where the bottom water temperature is around 0°C and in areas with periodically sea ice cover (Steinsund et al., 1994).

3.4.2.7. Trifarina angulosa (Williamson, 1858)

Trifarina angulosa lives infaunal and is restricted to coarse sediments winnowed by strong bottom currents of Atlantic water masses (Mackensen et al., 1985). It has been proven that *T. angulosa* thrives in the Barents Sea when the water temperature is above 5°C and salinities

around 35‰ (Hald and Steinsund, 1992; Steinsund et al., 1994). The abundance of this specie can be used as an indicator of Atlantic Water in the paleoceanographical record (Steinsund et al., 1994).

Millionella subrotunda and *Triloculina trihedral* is found in high abundance in just one sample, and will not be included in the description, just mentioned in the results and discussion.

4. Results

In this chapter the results from gravity core HH13-243 GC will be presented and described. The sedimentology, foraminiferal distribution and stable isotopes will be presented separately and described in stratigraphic order from the oldest to the youngest. The core is 583 cm long, retrieved from the slide scar in the southern part of the Bear Island Trough Mouth Fan.

4.1. Sedimentological description

The core is divided into five lithological units (Unit 1-5) based on visual description, X-ray photographs, grain size distribution and variations in physical properties (Figure 4 and 5).

The lithological log is based on colour images, X-ray photographs and the grain size distribution. After opening, black spots, interpreted as sulphide tracers caused by bacteria during sulphide reduction (Forwick, 2001). They were observable for a few days before they disappeared. The log, including colour images of the sediment surface and X-ray photographs, are presented in figure 4 and 5. Fined-grained sediments dominate the lithology, with abundance of coarser material and shell fragments. The core is relatively homogenous except from big colour changes, layering and clasts in the lowermost section of the core. These changes are visible on the colour images and can be observed in the X-ray photograph due to density changes (Figure 5).

The physical properties of the sediments include the water content (%), wet bulk density (g/cm^3) and the magnetic susceptibility (10^{-5}SI). Measurements from the top, bottom and at the section boundaries are removed as they occasionally show abnormally high or low values. The water content shows a normal trend of down-core decrease due to the effect of sediment consolidation, with peaks to lower values in areas containing coarser material. The density increases evenly down the core from 1.5 to 2.1 g/cm^3. The magnetic susceptibility varies throughout the core with values ranging from 6 to $42*10^{-5}$SI.

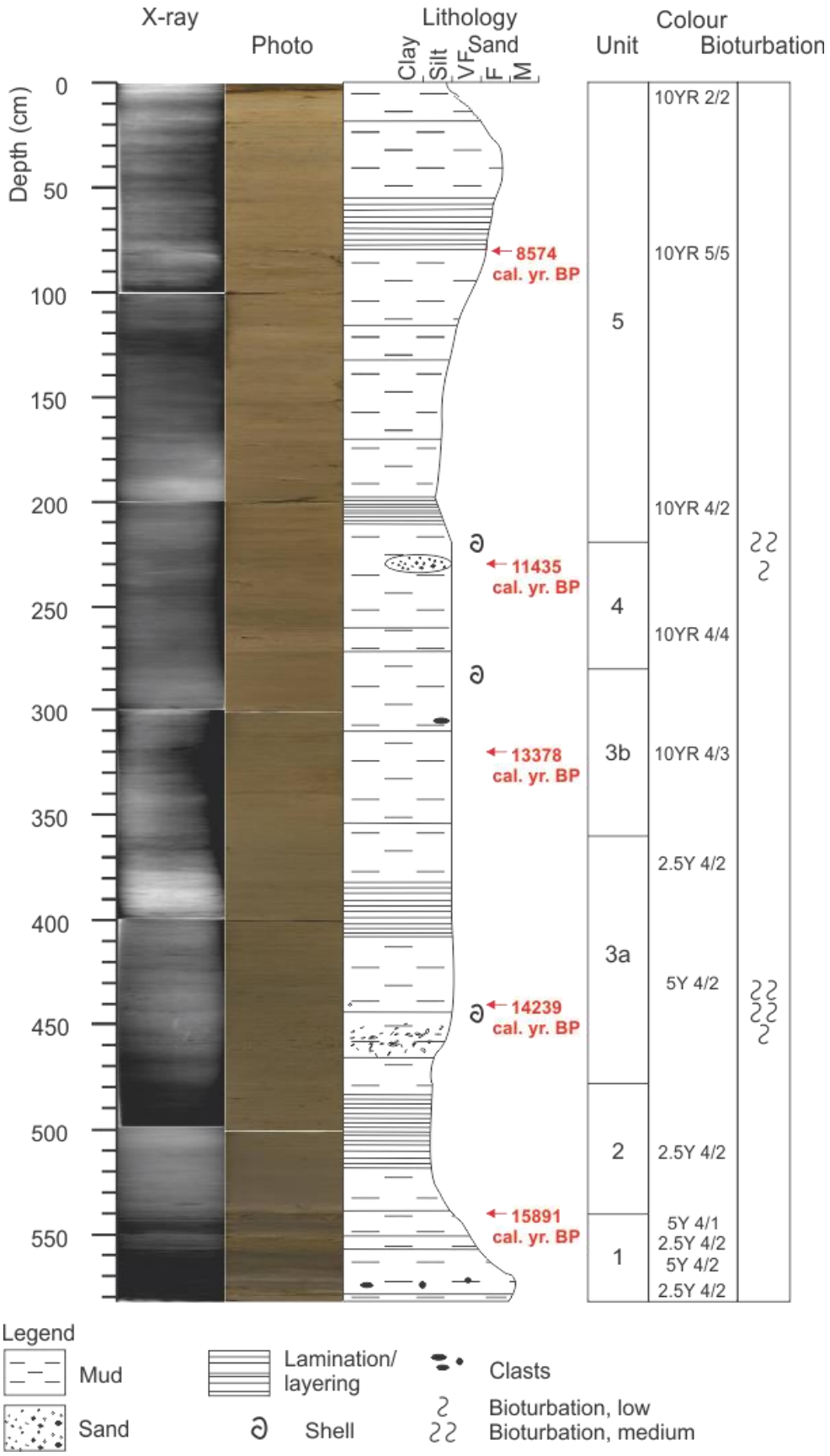

Figure 3: Lithological log of core HH13-243 GC showing X-ray image, sediment colour image, lithological units, Munsell colour codes, bioturbation and structures. The dated intervals, presented in calibrated years before present, are indicated by red arrows

4.1.1. Unit 1 (583-540 cm)

The lower most unit occurs between 583-540 cm and consists of diamicton (Figure 4). The sediment varies in colour with alternating dark greyish brown, olive brown, dark grey and olive grey layers (2.5Y 4/2, 5Y 4/2, 2.5Y 4/2, 5Y 4/1, respectively) (Figure 4). The diamicton comprise of partly laminated muds with coarse material spread throughout the muddy matrix. Size fraction <63um is really low and consist of only 4% in the 570-560cm interval, while the larger grain sizes dominate (Figure 5).

The unit is characterised by a high IRD content, and are most abundant between 570-560 cm with >1500 grains. Unit 1 have low magnetic susceptibility with only $10*10^{-5}$SI and water content fluctuates with an average of 25%, which is the lowest in the sediment core. The upper boundary of this unit at 540 cm is defined by a sharp possibly erosive boundary. The boundaries marks a clear change in both colour and grain size.

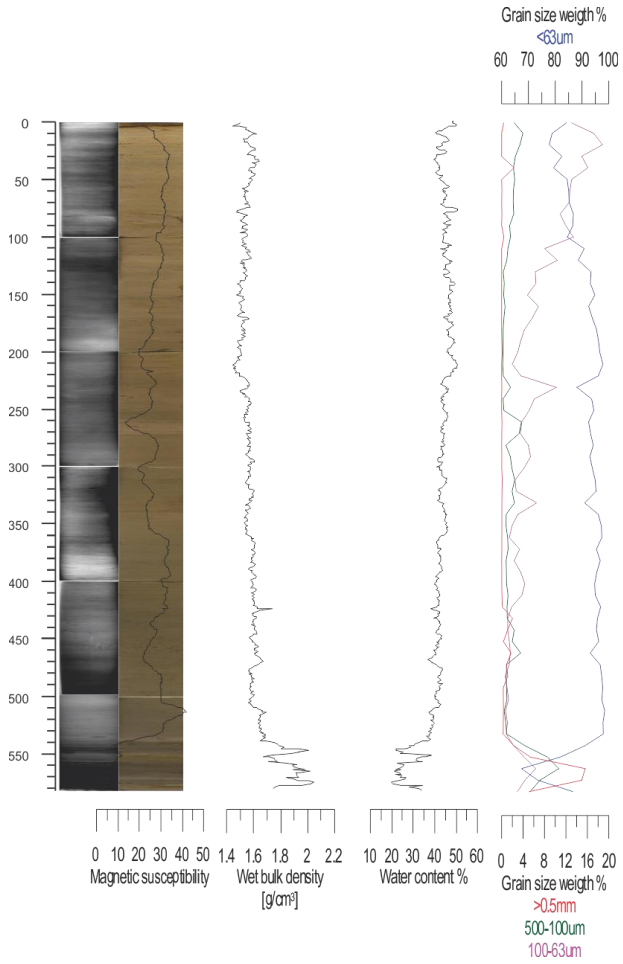

Figure 4: Log showing the X- ray image, colour photograph, magnetic susceptibility, wet bult density,water content and grain size of core HH13-243 GC

4.1.2. Unit 2 (540- 478 cm)

From the boundary of Unit 1 the grain size becomes more persistent homogenous with an increase in <63 um up to 97% and a colour change to more dark greyish brown (2,5Y 4,2). The sediments are well sorted and can from the X-ray photograph show some wavy structures from 540-510 cm before it become more laminated at 510 to 478 cm. The magnetic susceptibility increases from $10*10^{-5}$SI to $30*10^{-5}$SI and stays relative steady except for one peak at 520 cm where it increases to $40*10^{-5}$SI.

4.1.3. Unit 3 (478-280 cm)

Unit 3 is divided into two subunits, as there is a clear increase in the water content of 5% between the subdivisions, a change in the magnetic susceptibility and an increase in the the amount of very fine and medium sand (Figure 5).

4.1.4. Unit 3a (478-360 cm)

The lithology of Unit 3a varies; with a portion of drop stones at 470 – 430 cm. The X-ray show marked layers with coarser sediments and laminations. The drop stones seems to come in pulses with higher amount of fine sand than the previous unit, and shows several traces of bioturbation. The colour remains stable except for one layer at 445 – 428 cm which is olive grey (5Y 4/2), while the unit colour is dark greyish brow (2.5Y 4/2). The overall trend in the values of water content and magnetic susceptibility in the unit is increasing. There is high abundance of shell fragments in the area with high bioturbation (Figure 4)

4.1.5. Unit 3b (360-280 cm)

Unit 3b is characterised with an increasing amount of very fine sand. The unit is massive with a change in colour from dark greyish brown (2.5Y 4/2) to a transition between dark brow/brown (10YR 4/3). Less drop stones compared to the previous unit. The water content and magnetic susceptibility is nearly consistent with values at 45% and $20*10^{-5}$SI, respectively.

4.1.6. Unit 4 (280-220)

Unit 4 consist of massive sediments with an increase in grain size. The unit starts of with an increase in medium/fine sand, changing to very fine sand containing up to 10% in the end of

the unit with an average of 5%. The biggest change happens at 270-260 cm, here the colour changes to dark yellowish brown (10YR 4/4) and the magnetic susceptibility decreases from approximately $28*10^{-5}$SI to $15*10^{-5}$SI, before it increases to $25*10^{-5}$SI again. This layer consists of a high amount of fine to medium sand (4%). Shell fragment are found at 280 and 240 cm in conjunction with bioturbation.

4.1.7. Unit 5 (220-0 cm)

There is an increasing trend in grain size in unit 5 where the grain size starts with very fine laminated mud to containing more sand in the very fine-fine sand fraction (Figure 4). The colour gradually gets lighter, changing from dark greyish brown (10YR 4/2) to greyish brown (10YR 5/5). On top of the core, the last 5 cm is characterized by muddy very dark brown (10YR 2/2) sediments. The <63um goes from 96% to 77% towards the top and the size fraction 100-63um reflects the changes and lies between 6-18 %, while the 500-100um lies around 2%. The IRD in this unit is low throughout the unit. Unit 5 is characterized by an increasing trend in the magnetic susceptibility, from 20-$33*10^{-5}$SI. The X-ray photography doesn't show any big changes. There are found several shell fragments at 190-170 cm and at the surface and between 220-190 cm the sediments are containing a lot of diatoms.

4.2.Foraminifera

A total of 53 calcareous benthic and 7 planktonic species were identified in 59 samples from core HH13-243GC representing a diverse and well-preserved assemblage. There will be a primary focus on the dominating benthic and planktic species. A total of 16 benthic species will be presented in the faunal description based on; (1) Their dominance throughout the core, (2) If they have any special environment preference which can be useful in the paleoreconstruction and (3) They must exhibit more than 5 % of the total fauna in a sample. The foraminiferal record is divided into 5 assemblage zones (Figure 6, 7 and 8), based on the distribution patterns of both benthic and planktic species. Figure 6 shows the distribution of the 6 planktic species, figure 7 and 8 shows the distribution of 15 of the benthic species, the density, flux and diversity of the fauna in the different samples. At 570 and 560 cm there are small quantities (less than 80 foraminifera) of foraminifera and is therefore considered as non-representative samples. See chapter 4 for description of background and ecology of the different species.

The boundaries of the biozones units correspond well with the lithological units, and will be interpreted and discussed together later in chapter 5.

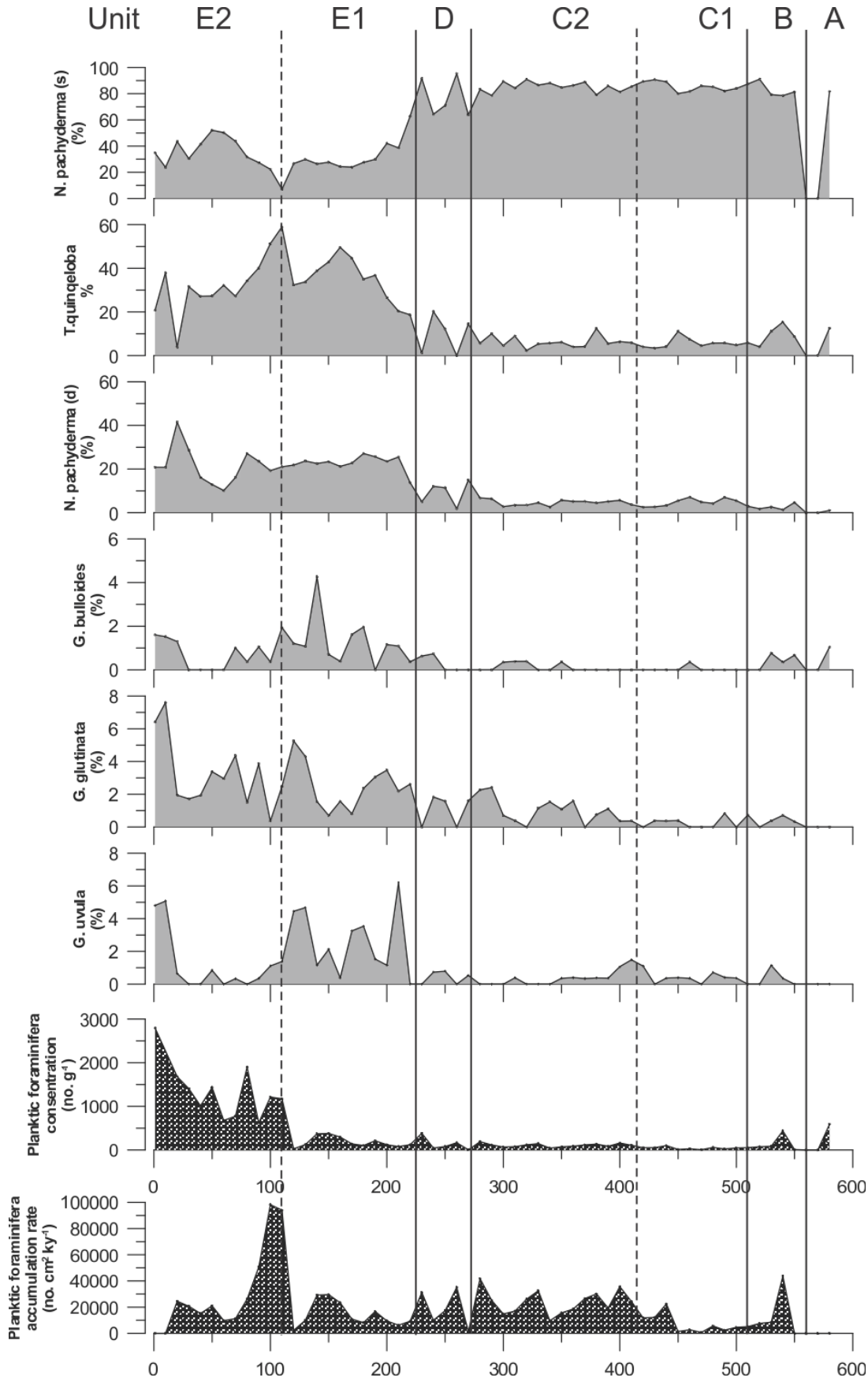

Figure 5: Planktic foraminiferal distribution (%) divided into units and plotted against depth (cm), together with the planktic foraminiferal concentration and accumulation rate (flux). The different faunal units are indicated on the figure.

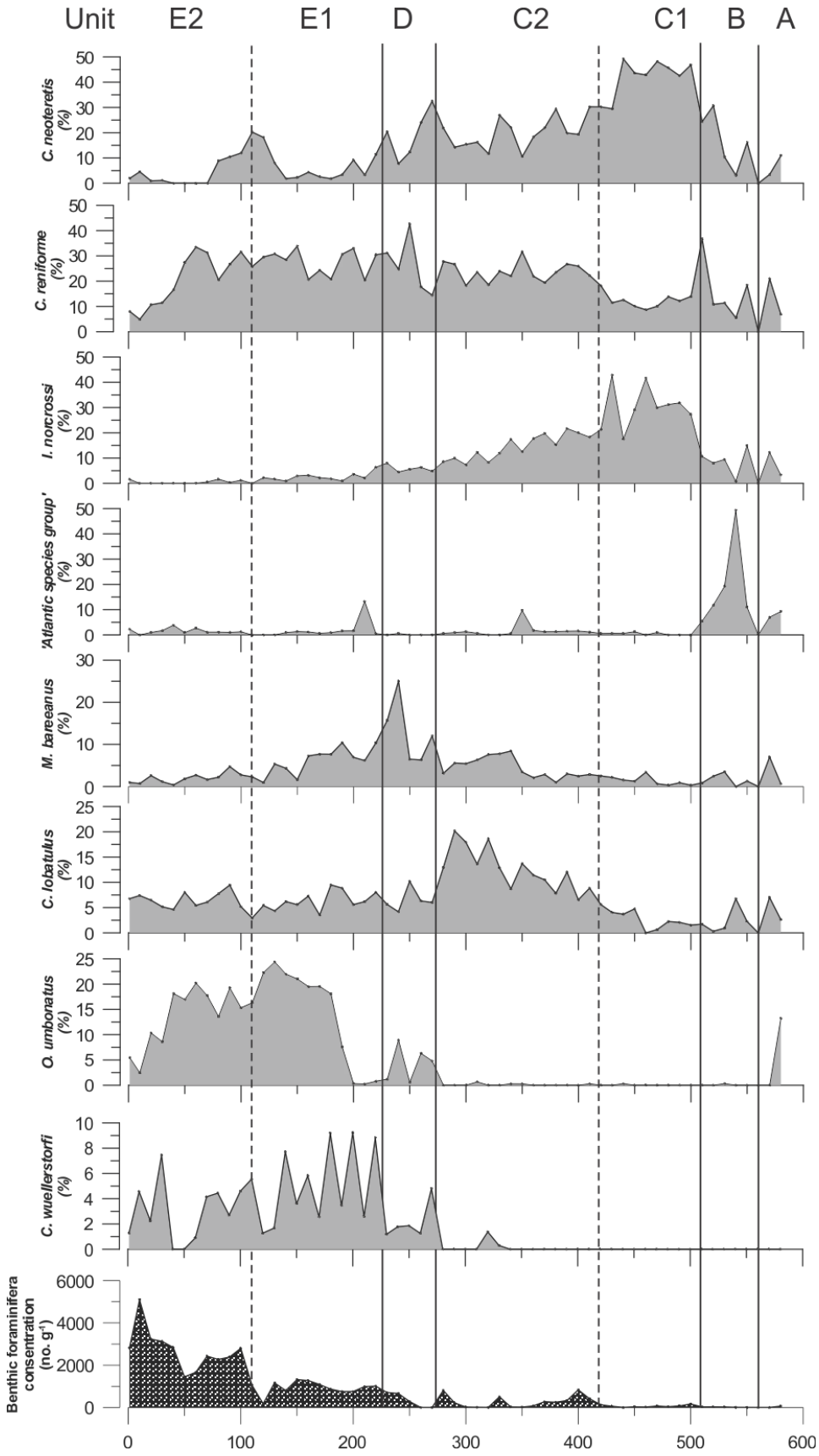

Figure 6: The dominated benthic foraminiferal distribution (%) divided into units and plotted against depth (cm), together with the benthic foraminiferal concentration. The different faunal units are indicated on the figure.

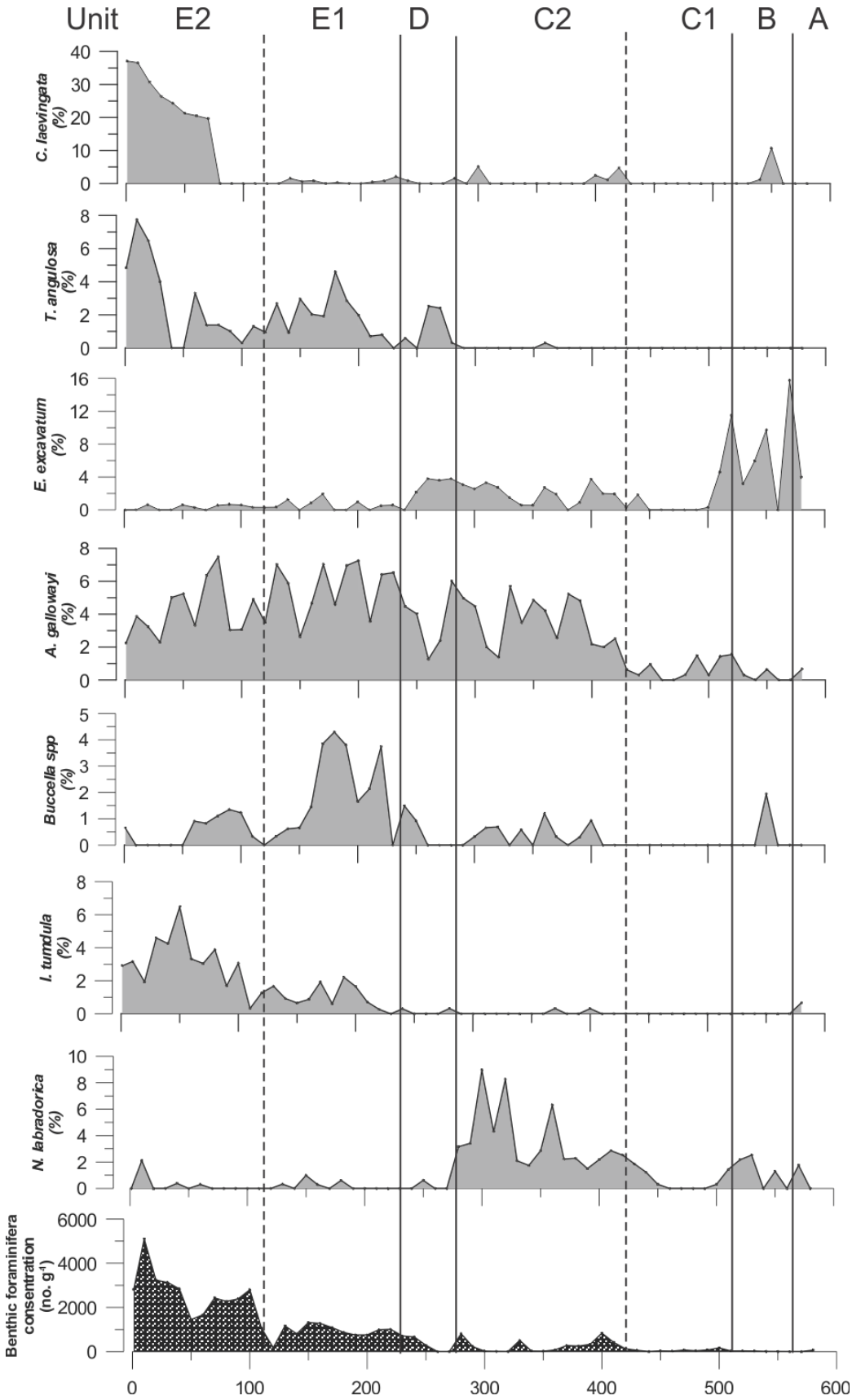

Figure 7: Sub-dominated benthic foraminiferal distribution (%) divided into units and plotted against depth (cm), together with the bentic foraminiferal concentration. The different faunal units are indicated on the figure.

4.2.1. Description of biozones

4.2.1.1. Unit A (583-560 cm) Neogloboquadrina pachyderma (s), Millionella subrotunda and Triloculina trihedral

The dominant planktic species is *Neogloboquadrina pachyderma (s)*, which constitutes 80% of the planktic fauna (Figure). Two of the dominating benthic species in this unit are the *Millionella subrotunda* with *26%* and *Triloculina trihedral* with 14%, which is the highest quantity of these species in the entire core; they are only abundant in small percentages at a few cm in the core. Because they are in small numbers in the rest of the core they are not included in the overview graphs. One other dominant species is the *Oridorsalis umbonata* witch consists of 13% of the total fauna in this unit. The subdominant species are *Cassidulina neoteretis, Elphidium exvavatum, Cassidulina reniforme, Pygro williamsoni* with respectively 11%, 10%, 7% and 7%. The foraminiferal flux of both benthic and planktic are low, while the diversity of species is high.

4.2.1.2. Unit B (560-510 cm) Neogloboquadrina pachyderma (s) and Atlantic species

In unit B the *Neogloboquadrina pachyderma (s)* still dominates the planktic fauna and increases from 80% to 90% of the total fauna. There is a smaller peak in the subpolar planktic species; *Turborotalita quinqueloba* with a notable percentage up to 15% (Figure 6).

In this unit the most prominent benthic feature is the abundance of *Atlantic species* that constituting up to 50% of the fauna at 540 cm (see chapter 4 for further explanation of the Atlantic species), *Bolivina sp.* has one peak which reaches 20% in the same sample. *Islandiella norcrossi sp., Cassidulina neoteretis/Cassidulina laevingata and Cassidulina reniforme* all dominates the fauna in the beginning and end of this unit; before and after the peak of *Atlantic species*. *Elphidium excavatum* is noteworthy in this unit with values between 3-11% and *Nonionella labradorica* with its 2%.

The planktic flux and concentration of foraminifera is moderate while the benthic flux is low. The diversity of species is the same as unit A (Figure 6 and 7).

4.2.1.3. Unit C (510-280 cm)

Unit C is dominated by the planktic species *Neogloboquadrina pachyderma (s)* with a sporadic occurrence of *Turborotalita quinqueloba, Neogloboquadrina pachyderma (d), Globigerina bulloides, Globigerinata glutinata* and *Globigerinita uvula.* The benthic fauna dominates of *C. neoteretis, I. norcrossi sp., C. reniforme and Cibicides lobatulus*. The unit is divided into subzones (C1 and C2) based on the occurrence of other benthic species and the change in the flux of benthic and planktic foraminifera.

4.2.1.4. Unit C1 (510-420 cm) Neogloboquadrina pachyderma (s), C. neoteretis and I. norcrossi

There is a big change in the benthic fauna at the boundary of this unit with an increase in *C. neoteretis* and *I.norcrossi,* where the occurrence of other species is minimal. Unit C1 has the highest abundance of *C. neoteretis* and *I. norcrossi* in the core reaching respectively 49% and 42% of the total fauna (Figure 7). The diversity of *C. reniforme, C. lobatulus* and *Melonis barleeanum* stays low, but stable throughout the unit (Figure 7).

The planktic and benthic flux is relative low, but starts to increase in the end of the unit. The diversity of forams decreases and is very low to the end of the unit where it starts to increase.

4.2.1.5. Unit C2 (420-280cm) Neogloboquadrina pachyderma (s), C.reniforme, C. neoteretis and C. lobatulus

The dominant species in Unit C1 starts to decrease and *C. neoteretis* has an average of 21% and *I. norcrossi sp.* 14% in unit C2. There is an increase of *C. reniforme* to an average of 25%, while *C. lobatulus* reaches its highest peak at 290cm and have an average of 18% of the total fauna. The diversity of species increases and gets higher compared to Unit C1. *Buccella spp.* has its first occurrence in this unit; which was total absent in C1. *M. barleeanus* is relatively constant at 5% and *E. excavatum* at 3%. *Astrononion gallowayi* varies in the unit, but have clear and higher peaks compared to unit C1 at 380-330cm and another one at 280cm. Where *A. gallowayi* has a larger drop at 320-310cm, *Nonion labradorica* have its highest peak in the core at 320-300cm and constitute 8% of the fauna. *Stanforthia spp*. has a peak with *N. labradorica* at 320 cm (Figure 8 and 14).

There is a decrease in the density of benthic species between 400-300cm with a small peak at 330cm; however, a large increase in the benthic flux dominates this unit. At 320 cm there is a low abundance of benthic compared to planktic. The density of planktic foraminifera is

relatively constant, whilst there is a high diversity of benthic foraminiferal species compare to the last unit.

4.2.1.6. Unit D (280-230cm) Neogloboquadrina pachyderma (s) C. reniforme

The unit begins with very low amounts of any benthic and some planktic foraminifera. Here the biggest changes are in the planktic assemblage, where there is a zigzag-shaped pattern in the *N. pachyderma (s).* It decreases where the amount of specimens are low to 64%, increases to 95%, then decreases to 64% and increases to 92%.

C. reniforme is the dominant specie in the unit with an average of 27%. *C. neoteretis* increases in the unit, before it decreases towards the end but have an average of 19% of the total fauna. *M. barleeanum* and *T. angolousa* increases with 15% and 2,5% towards the end of the unit, with a decrease in *C. lobatulus* and *A. gallowayi*. *N. labradorica* is absent in the fauna and *I. norcrossi* and *E. exavatum* is relatively constant at 7% and 4%.

4.2.1.7. Unit E1 (230-0cm)

There is a distinct change in the transition between Unit D and Unit E in the benthic and planktic fauna. The transition marks the first occurrence of *Cibicides wullestorfi* with some other species, and with a big sudden drop in *N. pachyderma (s).* Unit E is divided in two based on the big change in the flux of the foraminifera and a smaller change in the fauna (Figure 6, 7 and 8).

4.2.1.8. Unit E1 (230-110cm) Turborotalita quinqueloba, Neogloboquadrina pachyderma (d), Oridosalis umbonata and C. reniforme.

Unit E1 stands out with a sudden drop of N. pachyderma (s) from approximately 80% to 30%. *Turborotalita quinqueloba* reflect the changes in N. pachyderma (s) and is accompanied by *Neogloboquadrina pachyderma (d),* which together represent 54% of the total fauna. *Globigerina bulloides, Globigerinata glutinata* and *Globigerinita uvula* are in higher numbers in this unit and is characterised by a high amplitude pattern (Figure 6).

At the start of Unit E1, *C. reniforme* dominates accompanied by *M. barleeanum* and *C. wullestorfi.* At 190 cm., *O. umbonata* starts to increase and becomes the dominant species with *C. reniforme.* *C.wullestrofi* and *A. gallowayi* have big zigzag-shaped changes and lying between 8% and 5%. *Trifarina angolosa* and *Buccella spp*. becomes more common and has

just been registered earlier by very low values and have in unit E1 their peak at 160 cm with 4%. *Ioanella tumidula* becomes a part of the fauna, but only in small quantities.

4.2.1.9. Unit E2 (110-0cm) T.quinqeloba, C. reniforme and O. umbonata

At the boundary between Unit E1 and E2 there is a drop in the N. pachyderma (s), where is reaches 7% and *T. quinqueloba* constitute 59% of the fauna. In the rest of Unit E2, *N. pachyderma* has an average of 32%. *T. quinqueloba* and *N. pachyderma (d)* consuetude respectively 34% and 20 % of the total planktic fauna. *G. uvula* and *G. bulloides* decreases compared to unit E1, while *G. glutinata* remains the same. The planktic flux is really high in the beginning of the unit, before it slightly decreases.

C. reniforme represent 23% of the fauna, but is substituted in the last 40 cm by *Cassudulina obtusa*. The amount of *O. umbonatus* is relatively high before it decreases with an average of 14%. During the last 40 cm there is an increase in *Epistominella exigua* and *T. angalousa* together with *Cassidulina laevingata and Cassidulina obtusa*. *A. gallowayi* is steady with an average of 4-5%, and *Ioanella tumidula* increases to 4%. There is a decrease in *M. barleeanus* and *C. neoteretis*. *C. lobatulus* and *C. wuellerstrofi* have approximately the same values as the last Unit. The benthic flux is like the planktic, really high in the beginning of the unit.

4.3.Stable isotope analysis

The stable isotope ($\delta^{18}O$ and $\delta^{13}C$) analysis were obtained from planktic and benthic foraminifera from core HH13-243GC (Figure). As mentioned in the methods chapter (chapter 2.7), the selected species are the planktic specie *N. pachyderma (s)*. Three benthic species where selected; *C. wullestorfi*, *C. lobatulus* and *C. neoteretis*. *C. wullestorfi* and *C. lobatulus* were meant to create a coherent record of the bottom water conditions; unfortunately some samples in the middle (230-270 cm) and the bottom (440-550 cm) are missing due to spill and to too little materials in the sample. The $\delta^{18}O$ record was also corrected for ice volume effects, and will show these and the not corrected ones. The stable isotopes results are divided into same units as the foraminifera (Figure 9).

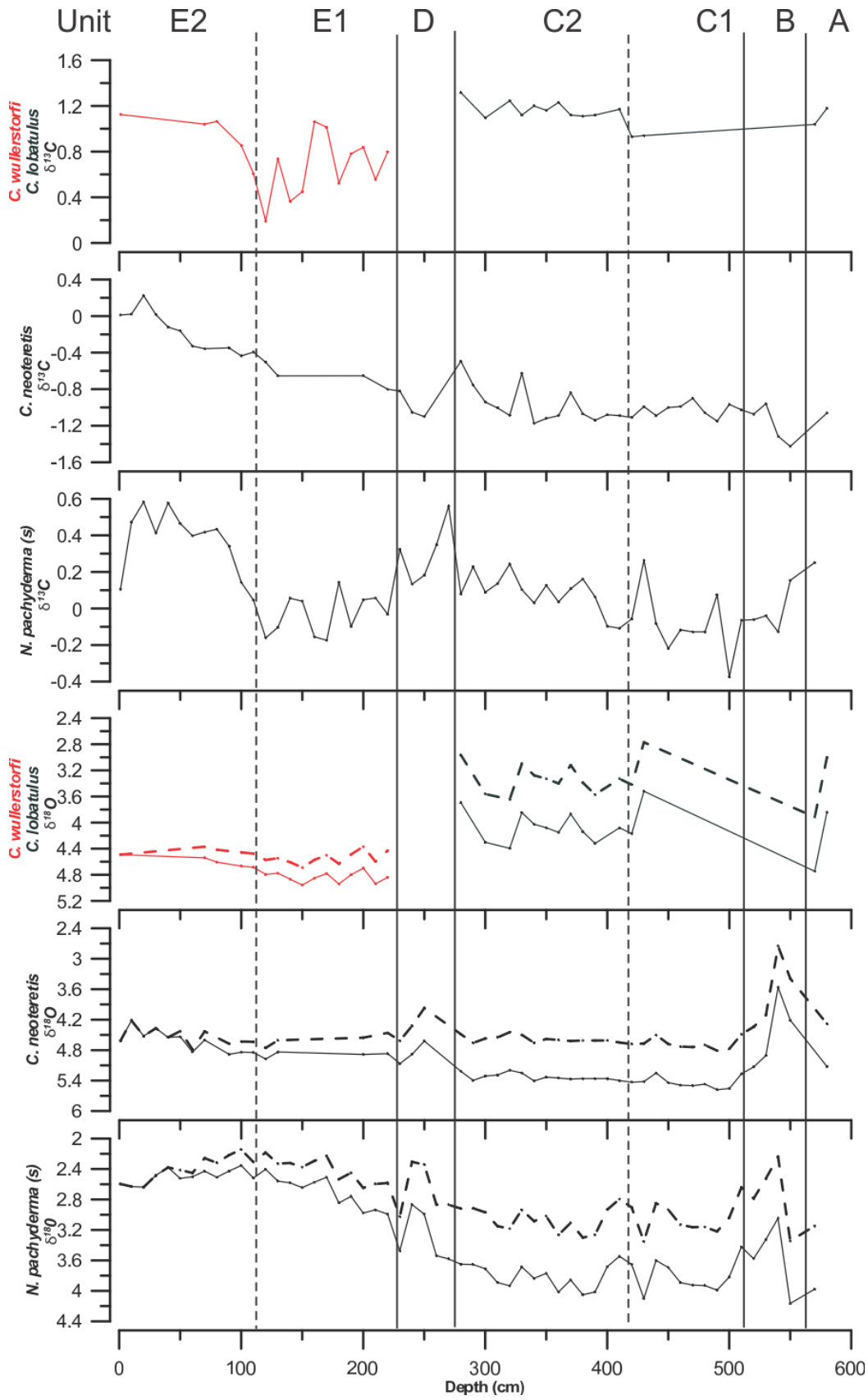

Figure 8: Measurements of stable isotopes of $\delta^{18}O$ and $\delta^{13}C$ for *N. pachyderma* (s), C. neoteretis, C. wuellerstorfi and C. lobatulus. The dotted lines indicate $\delta^{18}O$ ice volume corrected values, the continued line are the uncorrected ones.

4.3.1. $\delta^{18}O$ and $\delta^{13}C$ record

All of the species seems to follow a similar pattern up-core in the $\delta^{18}O$ and $\delta^{13}C$ record. The planktic $\delta^{18}O$ values for *N. pachyderma (s)* fluctuate from 2,3‰ to 4,17‰ within the core, with an average of 3,26‰, and the $\delta^{13}C$ varies from -0,37‰ to 0,58‰ with an average of 0,11‰. $\delta^{18}O$ for *C. neoteretis* range from 3,56‰ to 5,58‰, with an average of 5,04‰, and the $\delta^{13}C$ varies from -1,43‰ to 0,22‰ with an average of -0,79‰. The values for the ice volume correction are somewhat lower. *C. lobatulus* only represent a small portion of the record from 430 to 280 cm, and *C. wullestrofi* represent the last 220 to 0 cm (Figure 9).

There are two distinct changes in the record with an abrupt change in $\delta^{18}O$ to lighter values during a short interval where $\delta^{13}C$ follow this with significantly more depleted values. The first change is recorded at 540-510 cm in the core with a sudden drop of 1,1‰ in the planktic $\delta^{18}O$ record, and a 1,3‰ change for the $\delta^{18}O$ *C. neoteretis.* The $\delta^{13}C$ of *N. pachyderma (s)* and *C. neoteretis* have a decrease of 0,4‰ during approximately the same interval (580- 510 cm) ranging from respectively 0,25‰ to -0,13‰; -1,43‰ to -0,96‰ (Figure 9).

The next interval (510 to 280 cm) is characteristic with slightly constant values in $\delta^{18}O$ and $\delta^{13}C$. The *N. pachyderma (s)* $\delta^{18}O$ has an average of 3,84‰. One value stands out at 430 cm with a minor increase to 4,10‰ in the $\delta^{18}O$ N. pachyderma (s), which is also mirrored in the $\delta^{18}O$ for *C. lobatulus* (Figure 9). $\delta^{18}O$ values for C. lobatulus (430 to 280 cm) have high amplitude changes with around 0,5‰ change at the highest. The $\delta^{13}C$ values for *C. lobatulus* show an increase ranging from 0.93‰ – 1,32‰ during this interval. The values for C. *neoteretis* are relatively constant.

The other interval with a marked low planktic $\delta^{18}O$ excursion is occurring at 280 to 230 cm in the sediment core. N. pachyderma (s) have a decrease of 0,67‰ (3,54‰-2.87‰). The $\delta^{13}C$ values also stands out with a decrease of 0,43‰ (0,56‰ – 0,13‰). Here there is a gap between *C.lobatulus* and *C.wullestrofi* in the $\delta^{18}O$ and $\delta^{13}C$ record; however, *C.neoteretis* show an abrupt transition to more negative values at 250cm, before it turns in a positive direction (Figure 9).

The planktic $\delta^{18}O$ values remain relatively constant after 230 cm, with a slowly transition to lighter values towards the top of the core, while the $\delta^{13}C$ value change for *N. pachyderma (s)* and *C. neoteretis* at 100 cm with a with approximately 0,4‰ for all (Figure). The $\delta^{18}O$ and

$\delta^{13}C$ values of *C. wullestorfi* are characterised by a high amplitude pattern with rapid shifts of more than 0,5‰.

4.4. Chronology and establishment of an age model

The chronology of HH13-243 GC is based on five AMS radiocarbon dates from the planktic foraminiferal species *N. pachyderma (s).* When working with sediment cores and looking at changes and events, it is important to get an accurate impression of the changes and be able to correlate different datasets with each other. The radiocarbon dates were calibrated into calibrated years before present (cal. yr. BP) simplicity to easy correlate with other dated events in the literature.

4.4.1. Age model

The CALIB 7.1.0 program (Stuvier and Reimer, 1993) and the calibration curve MARINE13 (Reimer et al., 2013) is used to calibrate the radiocarbon dates to calibrated years before present. This program uses a global reservoir correction of 405 years. No regional correction (ΔR=0) was used. The chronology for the age model is established using the calibrated ages with the highest probability within the mean values of the σ2 range. The dates range from 80 cm to 540 cm in the core, leaving the bottom and top of the core with no radiocarbon dates, this because of insufficient material. The top of the core is assumed recent because of the colouring that indicates oxidization over time with sufficient environments for agglutinated foraminifera. The calibrated dates from core HH13-243 GC ranges from 15 891 cal. yr. BP to 8574 cal. yr. BP (Table 3).

The calibrated dates were plotted against depth to show an age model of HH13-243 GC (Figure 10), by assuming a linear accumulation rate between the dated levels. All ages presented in the following text will be presented as calibrated yr. BP.

Table 3: Details of the samples sent for radiocarbon dating, showing the mean age used for the age model for HH13-243 GC.

Lab reference	Core	Sampling depth (cm)	Species	14C age BP	Cal.yr BP 1 σ range	Cal.yr BP 2 σ range	Cal.yr BP 2 σ mean
UBA-32668	HH13-243GC	80-81	N. pachy s	8113± 37	8521-8624	8456-8698	8574
UBA-32669	HH13-243GC	230-231	N. pachy s	10377 ± 48	11278-11555	11231-11714	11435
UBA-32670	HH13-243GC	320-321	N. pachy s	11926 ± 46	13321-13432	13270-13491	13378
UBA-32671	HH13-243GC	440-441	N. pachy s	12706 ± 49	14101-14340	14044-14590	14239
UBA-32672	HH13-243GC	540-541	N. pachy s	13625 ± 53	15788-15990	15703-16084	15891

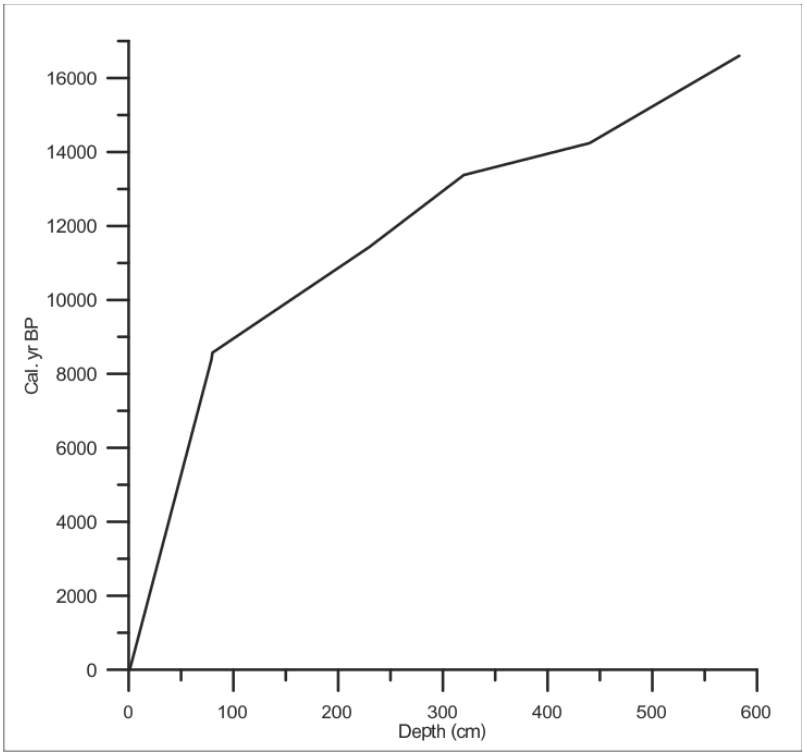

Figure 9: Age model with age in calender years plotted against core depth, assuming linear sedimentation rates betwwen the data points.

4.4.2. Sedimentation rate

The sedimentation rate witch is the accumulated centimetres of sediment per 1000 years, is calculated for each dated interval. The sedimentation between the dated intervals is assumed to be constant, so the linear sedimentation rate was estimated from the age and depth between the intervals (Table 4).

The average sedimentation rate for core HH13-243 GC is 61,61 cm/kyr varying between 9,39 and 139,37 cm/kyr. This correlates well with core T-88-2 (Hald and Aspeli, 1997) from approximately the same area within the slide scar, which has an average of 58,53 cm/kyr.

The highest sedimentation rate is 139,37 cm/kyr and is dated to have occurred between 14 239 to 13 378 cal. yr. BP. While the lowest sedimentation rate with 9,39 cm/kyr covers the top of the core.

Table 4: Showing the calculated linear sedimentationrates between the calibrated dates.

Interval (cm)	Interval (age)	Sedimentation rate (cm/ka)
0-80,5	0-8574	9,39
80,5-230,5	8574-11435	52,43
230,5-320,5	11435-13378	46,32
320,5-440,5	13378-14239	139,37
440,5-540,5	14239-15891	60,53

5. Interpretation and Discussion

In this chapter, the studied sediment core HH13-243 GC will be interpreted and discussed. The record will be discussed concerning the reconstruction of the paleoceanography in the studied area based on lithological changes, sedimentation rates, IRD content, foraminiferal assemblage, stable isotopes, physical parameters and the assumed age model (Figure 11, 12, 13, 14 and 15, respectively). These were also included when dividing the divisions into six main time intervals describing the paleoceanographic changes of the study area. The dates and the boundaries were approximated using the age model with assuming constant sedimentation rate between the dates. The oldest sediment within core HH13-243 GC suggest an age older than ~16 000 cal. yr. BP, suggesting that the core sediments were deposited during the last 16 000 years from the deglaciation to present.

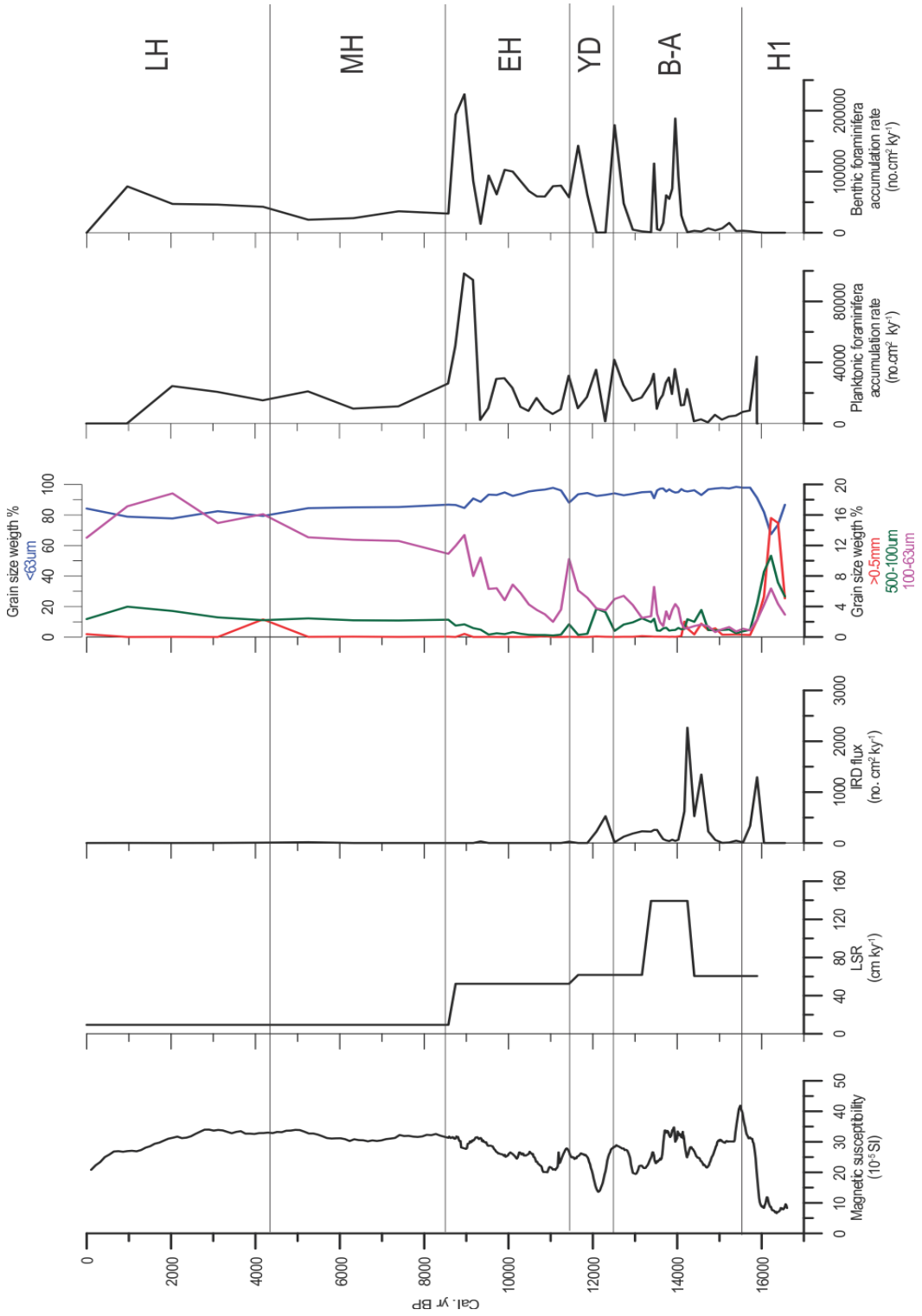

Figure 10: Proxy data for HH13-243 GC. The cal. yr BP plotted against the magnetic susceptibility, linear sedimentation rate, IRD flux, grain size distribution and the accumulation rate for planktic and benthic foramionifera with respect to the time intervals. Heinrich event (H1), Bølling-Allerød interstadial (B-A), Younger Dryas (YD), Early Holocene (EA), Mid Holocene (MH), Late Holocene (LH).

5.1.Heinrich event H1 (- ~15 500 cal. yr. BP)

Based on the age model, this period is interpreted to be a part of the end of Heinrich event 1 (H1). The sediments from H1 are in core HH13-243 GC represented by partly laminated sediments with relatively high flux of IRD, consisting of various grain sizes and a high diversity of benthic foraminiferal species with a southern affinity.

During the H1 the sea surface temperatures were low based on the dominance of the polar species *N. pachyderma (s)* (Bé and Tolderlund, 1971). (Figure 12). The core starts of with a few cm of very fine mud, before high amount of IRD and foraminiferal barren sediments were deposited. The benthic fauna in the very fine mud was dominated by *Milionella subrotunda, Triloculina trihedral, O. umbonatus* together with a smaller percentage of *Pygro* williamsoni, *C. neoteretis* and *C. reniforme*. The fauna indicates presence of warm but slightly chilled Atlantic water (Steinsund et al., 1994). The faunal composition and the sediments may indicate a glaciomarine environment with ice covered sea-surface due to the absence of lager clasts (Steinsund et al., 1994). The sediments with no foraminifera shift in colour, consisting of partly laminated mud with a high sand content and clasts (Figure 4 and 11). This could be due to influence of melt water plumes, down slope gravity flows or sediments transported by ice-berg/sea ice (Lekens et al., 2005). A minor increase in relative abundance of the planktic foraminifera *T. quinqueloba* indicates influence of Arctic surface water and chilled Atlantic water (Johannessen et al., 1994). A large shift in the benthic fauna occurs to higher abundance of the 'Atlantic species group'. The presence of 'Atlantic species' indicates that the bottom water was relatively warm (cf. Rasmussen et al., 1996a,b; Rasmussen and Thomsen, 2004). The high amount of Atlantic species (~50%) found in core HH13-243 GC from a water depth of approximately 1400 meter is unusual/unique as not any comparable high percentage has been found so far north before. Further north, Rasmussen et al. (2007) found that the 'Atlantic species group' constituted up to >25% on the shelf and 4-7% on the slope in two cores 76°N south west of Storfjorden from 389 m and 1485 m water depth, respectively. Above 80°N they are found to constitute 0-6% of the benthic fauna at the upper slope of Southern Yermark Plateau (Chauhan et al., 2014). We have to go further south to find a comparable high percentage, at approximately 63°N of the continental margin of Faeroe Island, a similar percentage of the 'Atlantic species group' is found and constituted up to 53% at a water depth of 1020 m (Rasmussen et al., 1996). Recent studies have interpreted that this group are occurring were there is bottom water warming due to prevented heat loss caused by meltwater and sea ice cover

(Duplessy et al., 1975; Rasmussen et al., 1996a; Rasmussen and Thomsen, 2004; Wullenburg et al., 2004).

Infaunal species have usually lower $\delta^{13}C$ values than epifaunal species, which is reflected in the results from *C. lobatulus*/*C. wuellerstorfi* compared to *C. neoteretis* (Figure 15). Foraminifera incorporate ^{13}C into their tests in equilibrium with the surrounding water, and the difference is interpreted to be a result of their microhabitat differences. Several studies confirm that this is due to remineralisation of organic matter within the sediment releasing ^{13}C- depleted CO_2 to the pore water (Grossman, 1987; Rathburn et al., 1996). The difference in the few measurements of *C. lobatulus* in the start of the record is 1.2‰ and -1‰ for *C. neoteretis*, but the overall differences can be observed in rest of the core (Figure 15). The large depletion in *N. pachyderma (s)* $\delta^{13}C$ values could be due to less primary production, less ventilation (more nutrients) or enhanced terrestrial carbon (Risebrobakken et al., 2010).

As long at this study does not provide any independent proxy record for temperature, it is difficult to distinguish whether the oxygen isotope signal reflects temperature or salinity changes. The isotope records show both the global ice volume corrected and the uncorrected values. The corrected values are depleted with 0.6 – 0.8‰, because the percent of ice in the system affect the oxygen isotope record by showing higher values in the worlds ocean. The ice volume is adjusted by subtracting the change $\delta^{18}O$ values due to sea-level change. This is based on the results where a 10 m sea level change (Grant et al., 2012) represent 0.11‰ change in the $\delta^{18}O$ signal (Fairbanks et al., 1989). But this is under the assumption that the ice volume changes were recorded at the same time globally, which is not the case.

The $\delta^{18}O$ values show a large decrease in *N. pachyderma (s)* and *C. neoteretis* (Figure 15). They record an up to -1.6‰ $\delta^{18}O$ excursion that spans the late phase of H1 (~15 500 cal. yr. BP). The low values of $\delta^{18}O$ in the planktic and benthic record are recorded in several other studies from the Barents Sea, Nordic Sea and the North Atlantic during the same time interval(Rasmussen et al., 1996, Dokken and Jansen, 1999, Rasmussen and Thomsen, 2004, Lekens et al., 2005). Dokken and Jansen (1999) proposed that the depletions in the benthic $\delta^{18}O$ signals are due to isotope-depleted brines formed due to sea ice formation. The formation of brines will take $\delta^{18}O$-depleted water with it as it sinks. The studied area has most likely been affected by different rate of sea ice formation, but it is not clear how it is recorded in the $\delta^{13}C$ and $\delta^{18}O$ record. Bauch et al. (2001) considered the same hypothesis and calculated that the rates of sea ice formation would have been unrealistically high and therefore unlikely.

Rasmussen and Thomsen (2010) have studied the brine formation in Storfjorden at Svalbard in the Barents Sea at present. The brines that reaches intermediate depth, is formed from cold, saline waters, not freshwaters, and have high $\delta^{13}C$ and $\delta^{18}O$ values. Other explanations could be warming of the intermediate water (Rasmussen and Thomsen, 2004, Ezat et al., 2014). Rasmussen and Thomsen (2004) suggest that relatively warm water enters the Nordic Seas at intermediate depths (<1700m), and flow below the low-salinity and low-density surface waters.

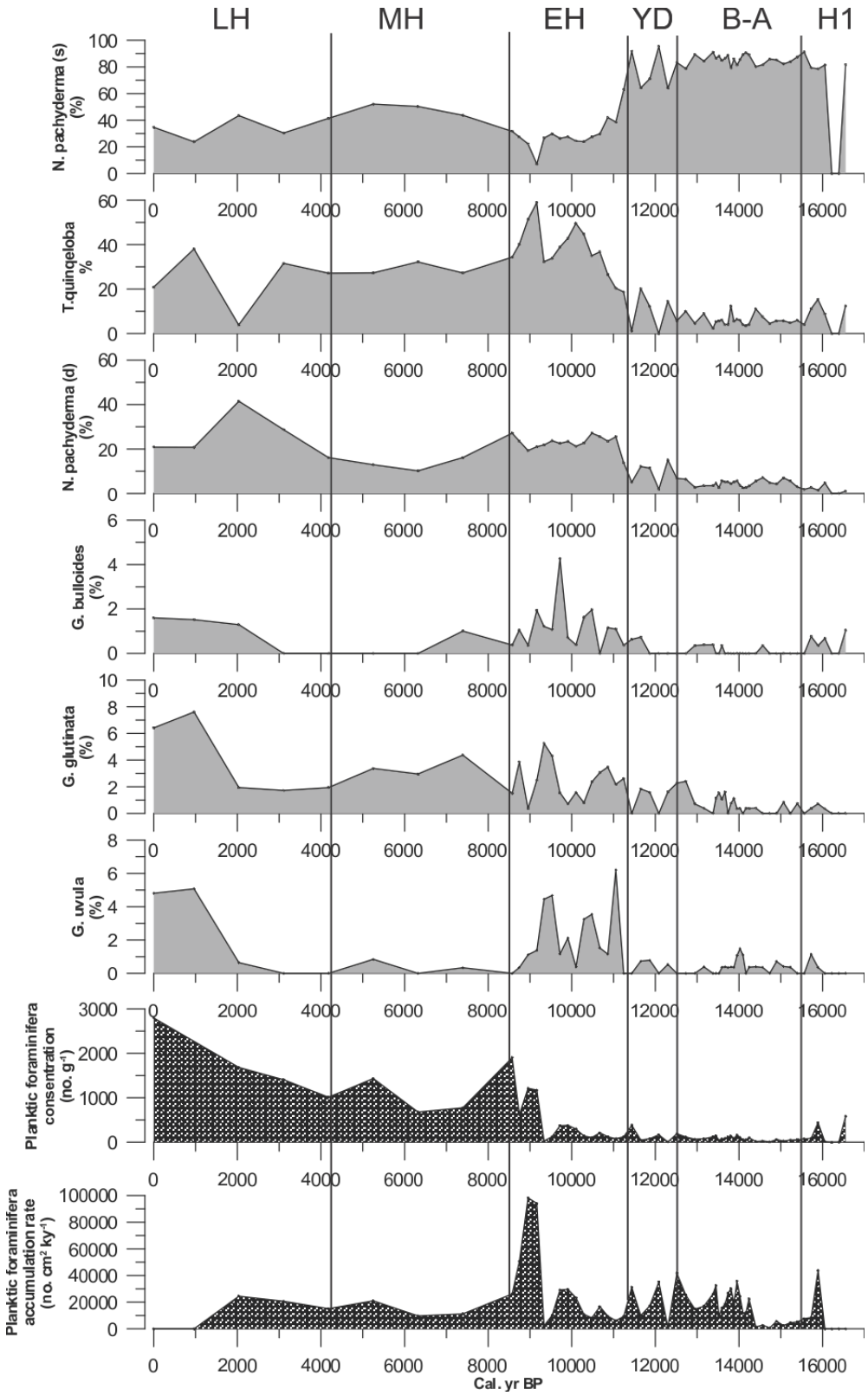

Figure 11: The planktic foraminiferal species, concentration and accumulation rate for the planktic foraminifera plotted against cal. yr. BP and divided into time intervals. Heinrich event (H1), Bølling-Allerød interstadial (B-A), Younger Dryas (YD), Early Holocene (EA), Mid Holocene (MH), Late Holocene (LH).

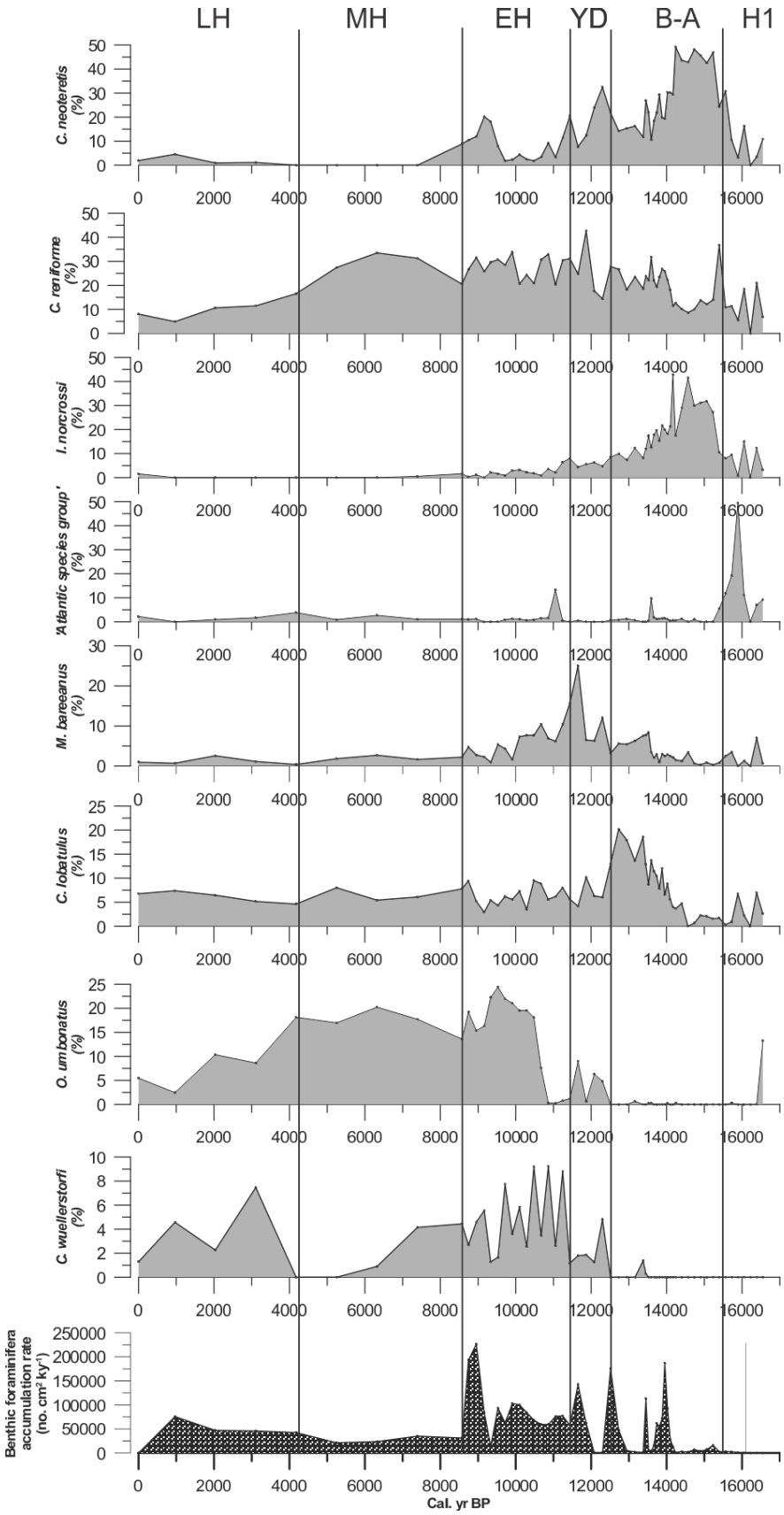

Figure 12: The dominated benthic foraminiferal species and accumulation rate for the benthic foraminifera plotted against cal. yr. BP and divided into time intervals. Heinrich event (H1), Bølling-Allerød interstadial (B-A), Younger Dryas (YD), Early Holocene (EA), Mid Holocene (MH), Late Holocene (LH).

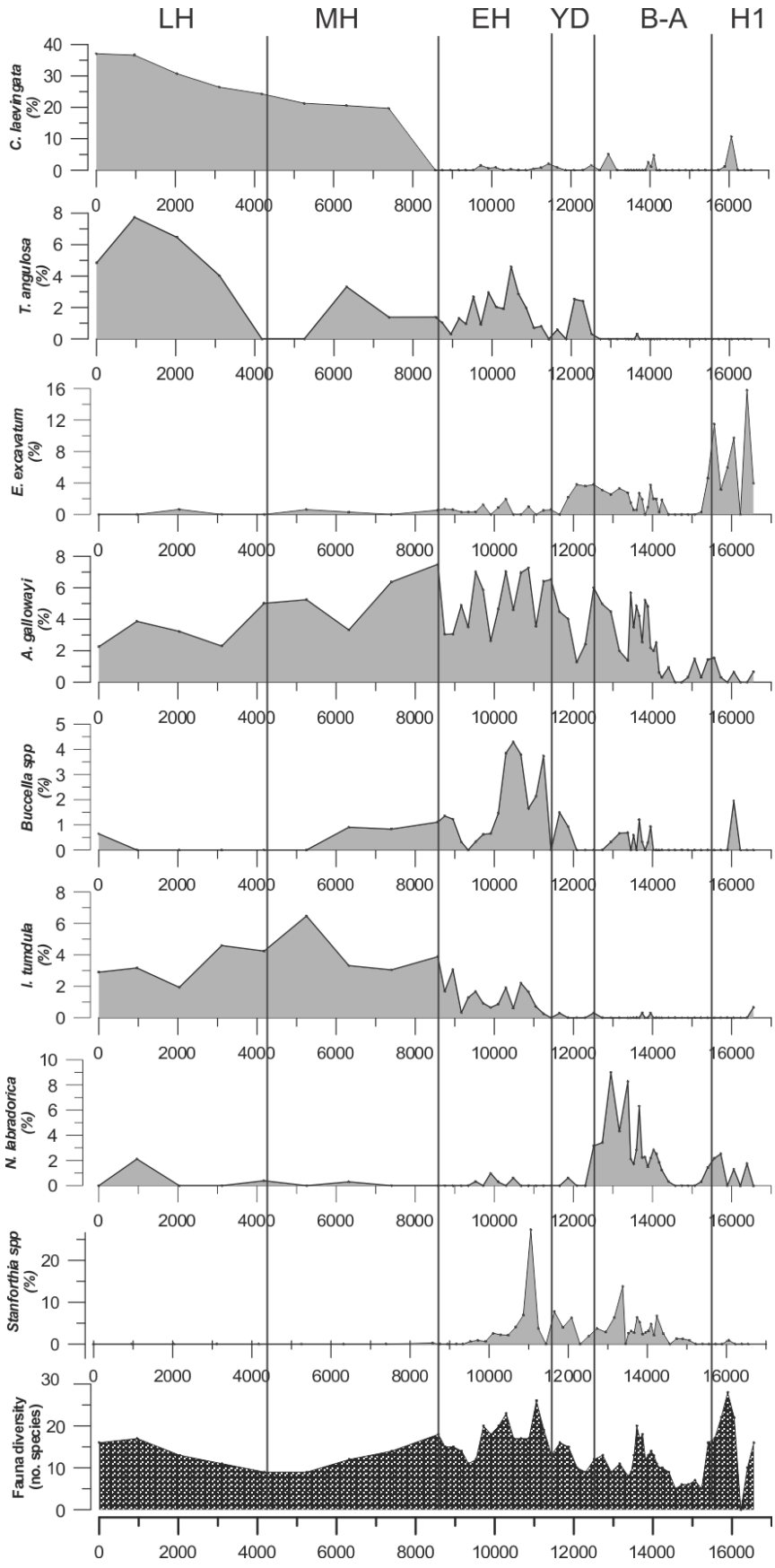

Figure 13: The sub-dominated benthic foraminiferal species and fauna diversity for the benthic foraminifera plotted against cal. yr. BP and divided into time intervals. Heinrich event (H1), Bølling-Allerød interstadial (B-A), Younger Dryas (YD), Early Holocene (EA), Mid Holocene (MH), Late Holocene (LH).

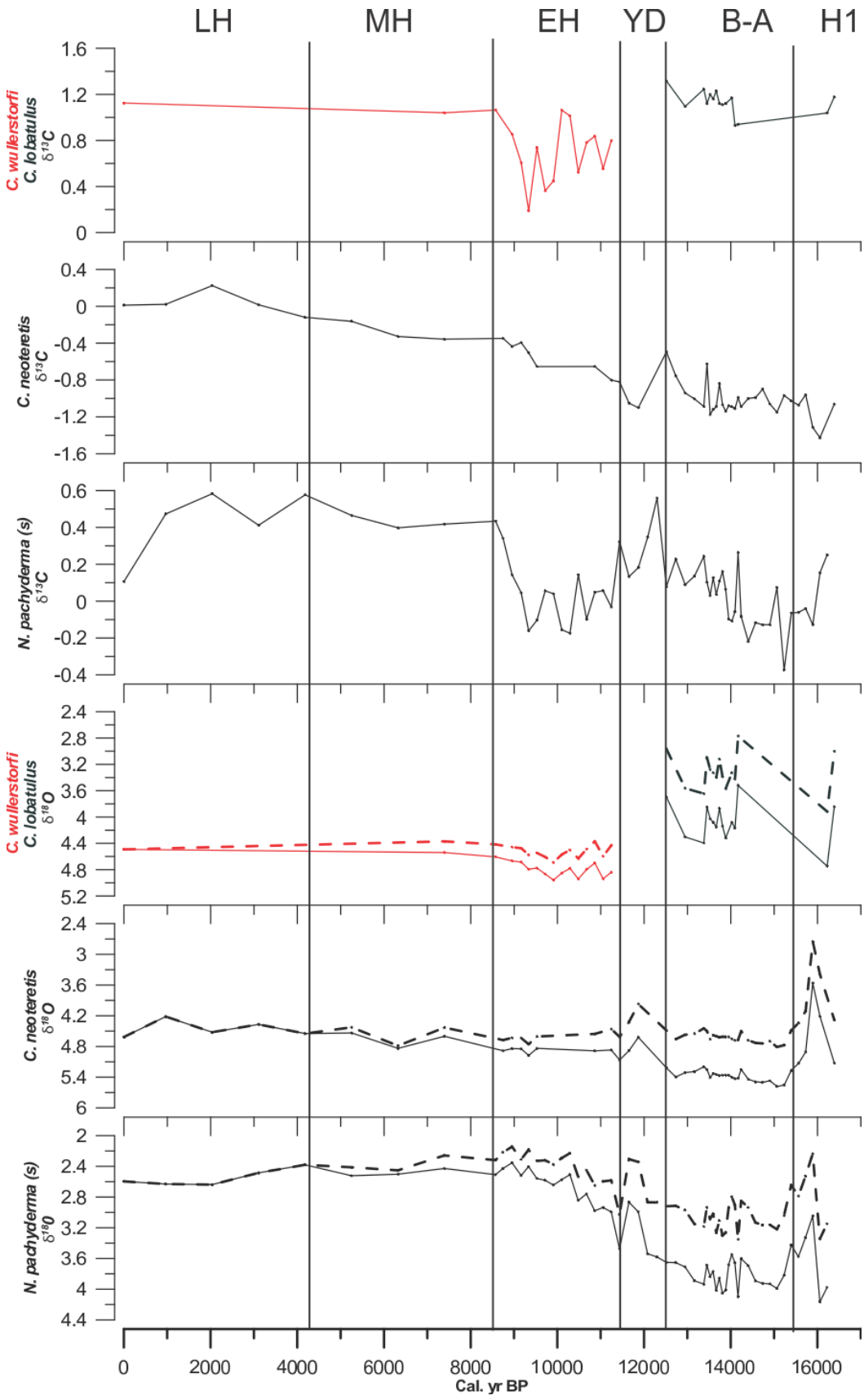

Figure 14: The stable isotopes for the planktic and benthic foraminiferal species plotted against cal. yr. BP and divided into time intervals. Heinrich event (H1), Bølling-Allerød interstadial (B-A), Younger Dryas (YD), Early Holocene (EA), Mid Holocene (MH), Late Holocene (LH). The dotted lines indicate $\delta^{18}O$ ice volume corrected values, the continued line are the uncorrected ones.

The large changes in the oxygen isotopes can be due to temperature or salinity changes. With the assumption that the oxygen isotope signal reflects temperature changes where 1‰ change reflect ~4°C temperature change (Duplessy et al., 1980) and with the presence of the 'Atlantic species group', we interpret that the change reflect temperature changes rather than salinity changes. Because of the species composition of the foraminiferal fauna and the relatively high flux of planktic foraminifera and IRD, it seems more likely. The results from core HH13-243 GC suggest that seasonally open conditions predominated in the studied area during H1, and that the H1 may reflect a 4-2 degree temperature change over a short time interval.

The characteristic of the sediments indicate that there were an increase in meltwater flow, and flux of icebergs/sea ice with high content of coarse material, since larger sand-sized grains are too heavy for current transportation (Bond et al., 1993). It is often complex to explain how IRD is transported to the sediments at the study site. They often have to be explained with other parameters as they cannot alone be explained by iceberg transportation. High concentrations and flux of IRD are often interpreted as an indication of increased calving of icebergs to the oceans (Jessen et al., 2010).

The peak in planktic flux and the low values of the planktic $\delta^{13}C$ and $\delta^{18}O$ (Figure 12 and 15 respectively) are interpreted to indicate melting of icebergs at the surface. The meltwater provided inorganic nutrients for growth of phytoplankton (Müller and Stein, 2014), and can explain the peak in the foraminiferal flux as an intensified planktonic productivity (Sztybor and Rasmussen, in press).

Earlier studies show that the deglaciation began 19 400 cal. yr. BP in Storfjordrenna north of Bjørnøyrenna (Rasmussen et al., 2007, Winsborrow et al., 2010, Aagaard-Sørensen et al., 2010), and at ca. 17 100 cal. yr. BP further south in Andfjorden, northern Norway (Vorren and Plassen, 2002, Winsborrow et al., 2010). Vorren and Kristoffersen (1986) and Andreassen et al. (2009) propose that the deglaciation of the SW Barents Sea started at ca. 15 500 cal. yr. BP. Recent studies investigating the deglaciation of the SW Barents Sea have detected traces of pronounced ice stream dynamics (Ottesen et al., 2005, Andreassen et al., 2008), where they have been divided into three specific flow events. The oldest flow extended to the shelf edge during the last glacial maximum (LGM) and an age of 18-16 ka BP has been suggested for this event (Vorren et al., 1990). The other two events are linked to the deglaciation, the second event terminated 100 km from the shelf edge, and represent an early readvance during deglaciation

(Andreassen et al., 2008) and is suggested to occur at 16 000 cal. yr. BP (Winsborrow et al., 2010).

This could explain the high peak in the IRD and coarser, partly laminated, foraminifera barren sediment at the bottom of core HH13-243 GC (Figure 11). There was high sediment transport of the ice streams, and Andreassen et al. (2008) found evidence that the ice streams existed through the final stages of the ice advance. The retreat was initiated within the deeper throughs, where the ice streams were most sensitive to ocean warming and sea level rise. In this manner the ice sheet would start to float as the deepest part were retreated, causing calving (Benn and Evans, 1998).

The decrease in *N. pachyderma (s)* may have been due to a small heating at the sub surface that may have triggered the Barents Sea Ice Stream in line with results from Marcott et al. (2011). According to their results and modelling results, subsurface warming could have acted as a trigger of continued release of icebergs from ice streams.

The partly laminations with alternating coarser sediments are interpreted to be a result of a suspension plume, based on the X-rays and grain size data (Hesse et al., 1997 and Cowan et al., 2001), initiated from the readvance of the ice sheets and active ice streams. The warm water benthic foraminiferal species and the minor decrease of *N. pachyderma (s)* could have affected the ice streams to retreat and thereby initiating calving.

5.2.Bølling-Allerød interstadial (15 400- 12 500 cal. yr. BP)

The laminated layer found in core HH13-243 GC have decreasing magnetic susceptibility with fine mud where the sediment rate is moderately high (60 cm ky^{-1}), before it increases to a very high magnitude (139 cm ky-1) (Figure 4 and 11). The laminated part is 35 cm thick deposited between 15 400 – 14 800 cal. yr. BP. This is approximately 500 years older than the dated laminated layer from Jessen et al. (2010). It spans over the same amount of years, the difference could be due to local reservoir age changes. The benthic and planktic foraminiferal flux is low(Figure 12 and 13), as is the benthic fauna diversity with just 5-6 species, which are dominated by *C. neoteretis*, *C. reniforme* and *I. norcrossi* (Figure 14 and 13 respectively). The faunal composition indicate presence of chilled Atlantic Water below cold and fresh polar waters, with high and stable bottom water salinities and seasonal sea-ice cover (Steinsund et al., 1994, Korsun and Hald, 1998, Polyak et al., 2002). The IRD and foraminifera poor laminated mud interval could indicate rapid sedimentation by suspension settling from seasonal

melt water plumes (Kneis et al., 2007) and extensive sea ice cover (Dowdeswell et al., 2000). *C. lobatulus* and *A. gallowayi* are current-indicator species (Steinsund et al., 1994, Wollenburg and Mackensen, 1998), the increase in the assemblage towards the latter part may indicate increased bottom current activity. As *C. lobatulus* is considered a shallow- water species it may be reworked. The high relative abundance of *C. neoteretis* indicates that there must be a constant inflow of Atlantic water in the area overlain by cold-water masses (Jennings et al., 2004). The Atlantic water created a high-energy regime with winnowing on the shallower part of the shelf (Hald and Aspeli, 1997). The winnowing may have caused down-slope transport and could explain the high amount of shallow water species and extremely high sedimentation rate. After the laminated layer the benthic faunal diversity slightly increase, and *E. exavatum* become more common, and indicate glaciomarine conditions (Hald and Korsun, 1997).

The Bølling - Allerød Interstadial comprised high amount of *C. neoteretis* in the beginning before it decreases towards the end (Figure 13). In the latter part, there seems to be a decrease in temperature of the incoming Atlantic water based on the benthic fauna. The relative abundance of *Stanforthia spp.* and *Buccella spp.* increases and *C. reniforme* becomes the most abundant species (Figure 13 and 14). They all prefer lower temperatures around freezing point (Steinsund et al., 1994). Right before the transition to Younger Dryas there is a peak in relative abundance of *N. labradorica*. This can indicate that an oceanic front was approaching the study site (Steinsund et al., 1994). The relative abundance of *E. excavatum* is moderate and often found in environments with high sedimentation rate and high turbidity. This supports the interpretation of relatively cold surface water as the species is exclusively confined to Arctic waters with winter sea ice cover. This coincides with results from other studies along the SW Barents Sea slope (Aagaard-Sørensen et al., 2010, Hald et al., 2007)

According to Sartheim et al. (2003) low $\delta^{13}C$ values in *N. pachyderma* (s) and *C. neoteretis* may indicate warm, but poorly ventilated Atlantic water. This can be recognized from the Barents Sea record, where the carbon isotopes are low during the deglacial warm phases and increases towards Younger Dryas. The $\delta^{13}C$ depletions can however also be interpreted as meltwater pulses, with highly unstable ventilation and reduced convectional processes, as observed by Bauch et al. (2001), just prior to and after the Younger Dryas.

5.3. Younger Dryas (12 500- 11 400 cal. yr. BP)

The Younger Dryas (YD) is a well-known cooling event in the North Atlantic region that started and ended abruptly (Ebbesen and Hald, 2004). Towards the Younger Dryas there was a decrease in relative abundance of *C. neoteretis*, which may as mentioned indicate a reduction or decrease in temperature of the incoming Atlantic water to the study area. Supported by the increase of the relative abundance of *Stainforthia spp* (Figure 14), which is associated with bottom water temperature around 0°C and seasonal sea-ice cover (Steinsund et al., 1994). The planktic foraminiferal assemblage is still dominated of *N. pachyderma (s)* indicating cold surface water conditions, with possible extensive sea-ice cover indicated by the lowered planktic and benthic foraminiferal flux. The increase in sea-ice cover and a reduced inflow of Atlantic water may also result in the reduction of winnowing at the banks, and in turn cause the lowered sedimentation rate (Hald and Aspeli, 1997).

During the Younger Dryas there is a change in the planktic foraminiferal fauna, and the relative abundance of *N. pachyderma* (s) decreases to 64% (Figure 12), and *T. quinqueloba* and *N. pachyderma* (d) constitute 30 %. *T. quinqueloba* is associated with the fertile Arctic surface water and oceanic fronts (Jennings et al., 2004), and may together with *N. labradorica* partly support the presence of mixing of water masses. This may in turn explain the increase in grain size distribution and IRD in this interval (Figure 11), which could be deposited from melting icebergs in warmer surface waters. After 12 000 cal. yr. BP the relative abundance of *C. reniforme* increases, and may indicate a subsurface inflow of chilled Atlantic water with lowered salinity (Hald and Steinsund, 1992, Ślubowska-Woldengen et al., 2008). *M. barleeanus* increases after ca.11 900 cal. yr. BP, which can indicate higher organic flux to the sea floor (Steinsund et al., 1994).

Throughout the entire YD, the abundance of *N. pachyderma* (s) is fluctuating in a seesaw pattern occurring between 94 – 64 – 92 % of the total fauna (Figure 12). The $\delta^{18}O$ values for *N. pachyderma* (s) show an abrupt change to lower values (Figure 15) during the Younger Dryas. The $\delta^{18}O$ values started to decrease after 13 000 cal. yr. BP, but at around 11 700 cal. yr. BP there is a 0.8-0.6‰ change over a relatively short interval. This is also seen in the benthic $\delta^{18}O$ record, but with a smaller magnitude (0.6-0.4‰). The change can as in H1 reflect either salinity or temperature change; the difference may be that the $\delta^{18}O$ values for *N. pachyderma* (s) in Younger Dryas reflect salinity changes due to fresh surface water rather than temperature change. Younger Dryas occurred during times of maximum insolation (Bauch et

al., 2001), and is known as a cooling event that from the Greenland ice cores show low cold air temperatures (Grootes et al., 1993).

The high $\delta^{13}C$ values observed in core HH13-243 GC during the first part of YD coincides with the accumulation of IRD, as well as cold surface water as seen by the increase in *N. pachyderma* (s). The high $\delta^{13}C$ values were also observed by Bauch et al. (2001), who interpreted the results as increased rates of vertical convection in the Nordic seas, and that the later depletion could imply a slowdown of this convection. The inferred lower rates of vertical convection during the depletions could have been caused by meltwater at the surface (Bauch et al., 2001). This melt water could explain the low $\delta^{18}O$ values at the end of the YD.

5.4.Early Holocene 11 400- 8500 cal. yr. BP

The first appearance of *C. wuellerstorfi* (Figure 13) may be a benthic response to the changes in the bottom and surface water conditions as it is related to interglacial conditions in the Nordic seas (Bauch et al., 2001) and increased nutrient supply in the Norwegian Sea (Mackensen et al., 1985). There is an abrupt change in the planktic assemblage at the transition from the Younger Dryas to the Early Holocene, as *N. pachyderma* (s) decreases to 20%, and *T. quinqueloba* and *N. pachyderma* (d) constitute 54 % of the total fauna (Figure 12), which indicate a large increase in the surface water temperature. *T. quinqueloba* is associated with an oceanic front where there is high nutrient supply, and *N. pachyderma* (d) is linked to the influx of Atlantic Water in the northern North Atlantic (Johannesen et la., 1994). The surface warming is supported by the high amount of diatoms *(Coscinodiscus spp.)* and the increase in relative abundance of *G. uvula*, *G. glutinata* and *G. bulloides* (Figure 12) which all thrives in relatively warm waters (Bé and Tolderlund, 1971, Hald et al., 2007). The diatoms are found between 230-190 cm in the studied core, with the highest amount around 220 cm, which is approximately at 11 054 cal. yr. BP. The diatoms were first described in the Fram Strait by Stabell (1986), where the diatom maximum is time transgressive and linked to the northward movement of the Polar front (Jansen et al., 1983; Stabell, 1986). In the south-eastern part of the Norwegian Sea the Polar front retreated northward at ca. 11 700 cal. yr. BP (Stabell, 1986; Koc-Karpuz and Jansen, 1992), which is almost 700-800 years earlier from core HH13-243 GC, and around 900 years before the diatoms appeard over the western Svalbard slope (Jessen et al., 2010). As mentioned, the dates in core HH13-243 GC are not corrected for regional reservoir age differences, so the diatom-rich layer could be closer in time with the western Svalbard slope. Towards the end of the Early Holocene at 9150 cal. yr. BP, *T. quinqueloba* dominates (59 %) the total fauna with

the highest accumulation rate for the planktic and benthic foraminifera recorded in the studied area (Figure 12 and 13). This may indicate that a southward movement of Arctic water influenced the site. This could cause a strong inflow of Atlantic water, change in nutrient supply due to the fronts, causing high productivity. The $\delta^{13}C$ and $\delta^{18}O$ record for both planktic and benthic foraminifera have fluctuating values throughout the entire Early Holocene. This is interpreted to be due to the presence of the Arctic front in the area and the mixing of different water masses. Low $\delta^{13}C$ and $\delta^{18}O$ of recent *N. pachyderma* (s) in surface waters is according to Johannesen et al. (1994) in the Norwegian Sea typical for warm Atlantic water. Concurrent with the planktic fauna the benthic fauna changed to a high diversity fauna with high abundance of *C. lobatulus* and *C. wuellerstorfi*, indicating a large influence from increased bottom currents (Hald and Steinsund, 1992). The secondary species of *Buccella spp*, *T. angulosa* and *I. tumidula* also clearly point to stronger influence from Atlantic water (Hald and Steinsund, 1992).

The planktic faunal shift at the transition between Younger Dryas and Early Holocene show clear indication of a shift in the surface waters, where Atlantic water replace Arctic Water at this time (Figure 12). The planktic assemblage dominated of *T. quinqeloba* and *N. pachyderma* (d) together with influx of *G. bulloides*, *G. uvula* and *G. glutinata*. The distribution of the diatoms, planktic and benthic foraminifera may indicate that strong frontal systems prevailed in the early Holocene close to the SW Barents Sea margin.

5.5.Middle Holocene 8500- 4200 cal. yr. BP

The benthic foraminiferal assemblage is dominated by *O. umbonatus*, *C. reniforme* and *M. barleeanus*(Figure 13), indicating stronger inflow of Atlantic water and a stable food supply (Hald and Steinsund, 1992). The sea surface temperature may indicate slightly colder conditions towards the Late Holocene as the relative abundance of *N. pachyderma* (s) increases, and *N. pachyderma* (d) and *G. bulloides* decrease. Hald et al. (2007) suggested that these cooling periods that occurred in the end of Early Holocene and through Mid Holocene were caused by increased influence of Arctic water. The inflow of Arctic water could be forced by southward displacement of Arctic Water from the north-eastern Barents Sea, due to less heat advection from the south (Hald et al., 2007). During the Early Holocene there is an increasing in the proportion of very fine sand fractions, which continues throughout the period and into the Late Holocene. The sediments consist of fine mud with little IRD and the sedimentation rate is relatively low, and resembles open ocean conditions with hemipelagic sedimentation and current transportation (Laberg et al., 2005). The flux of planktic and benthic foraminifera is

stable, but lower than the Early Holocene. The oxygen isotope values are quite stable, while the carbon isotope values slightly increases (Figure 15).

During the Mid Holocene, the Fram Strait development in water-mass/sea-ice conditions were comparable to the modern situation, considering the in- and outflow of Atlantic (WSC) and Polar waters (EGC), respectively (Bauch et al., 2001). The $\delta^{13}C$ values increase throughout the rest of the Holocene, and reaches the highest values, which can be explained by the environments we find in the Arctic ocean today (Bauch et al., 2001), which may indicate an increase in oxygenation and more nutrient depleted waters.

5.6.Late Holocene 4200 – 0 cal. yr. BP

The late Holocene represents just the top most 40 cm of the sediment core. The core top is interpreted to be 0 years due to the colouring of the sediments, which is dark reddish- brownish, and containing abundant agglutinated specimens. The sediments get this dark reddish colour due to oxidization of the subsurface, and indicate no disturbance of the sediments during the coring process (Rasmussen's personal comment). The fauna indicates that we have the same assemblage that is found in the deep sea today. The modern foraminiferal faunas on the slope of the Southwestern Barents Sea is dominated by the planktic foraminiferal species *N. pachyderma* (s), *N. pachyderma* (d), *T. quinqueloba, G. bulloides, G. uvula* and *G. glutinata* (Hald et al., 2007) (Figure 12). On the slope at water depths below ca. 1200 m, *C. wuellerstorfi, E. exigua, I. tumidula* and *O. umbonatus* becomes common (Mackensen et al., 1985; Rasmussen et al., 2007) (Figure 13 and 14). The combined planktic foraminifera assemblage of *N. pachyderma* (d) and *N. pachyderma* (s), suggest warm surface water and colder subsurface.

6. Summary and conclusion

The study of planktic and benthic foraminifera, isotopes and sediments from the sediment core HH13-243 GC show the paleoceanographic changes that prevailed over the Bear Island slide scar during the last Deglaciation and Holocene. The results and the main outcomes from this study are described as follows:

The results from core HH13-243 GC suggest that seasonally open conditions predominated in the studied area during H1 (- ~15 500 cal. yr. BP), and that the H1 may reflect a 4-2 degree temperature change over a short time interval. During the H1 the benthic foraminiferal fauna is dominated by 'Atlantic species' that indicate warm bottom water under cold surface waters.

Based on the age model, the lowermost sediments in core HH13-243 GC is older than ~15 891 cal. yr. BP and fall within the latest part of the Heinrich event 1. The coarse, foraminifera-barren sediments were deposited under cold glacial conditions in the proximity of an active ice sheet.

The foraminiferal abundance indicate that the surface waters in H1 was cold, however, a slight warming of the subsurface could have initiated a further retreat of an active ice stream in the Barents Sea.

During the Bølling-Allerød interstadial there was a continuous inflow of Atlantic water to the study area, which towards the latter part indicated colder conditions with chilled Atlantic water and extensive sea-ice cover.

Prior to the Younger Dryas, the surface ocean warmed by the increase abundance of subpolar planktic foraminiferal species. The Younger Dryas is defined in this study to a shift in the benthic and planktic foraminiferal faunas, from predominantly warm-water species to cold-water species.

The abrupt transition from polar to subpolar planktic foraminiferal fauna at the core site falls within the onset of Holocene conditions at 11 200 cal. yr. BP, associated with enhanced influence of Atlantic water at the sea surface.

The distribution of diatoms, planktic and benthic foraminifera may indicate that strong frontal systems prevailed the early Holocene close to the SW Barents Sea margin.

The Mid Holocene is characterized by several cooling events, where inflow of Arctic water influences the sea surface.

During the late Holocene we get a similar fauna assemblage that is found in the deep sea today. The modern foraminiferal faunas on the slope of the Southwestern Barents Sea is dominated by the planktic foraminiferal specie *N. pachyderma (s), N. pachyderma (d), T. quinqueloba, G. bulloides, G. uvula* and *G. glutinata*. On the slope at water depths below ca. 1200 m, *C. wuellerstorfi, E. exigua, I. tumdula* and *O. umbonatus* dominates, which suggest warm surface water and colder subsurface.

7. References

Alley, R. B. 2007. Wally was right: predictive ability of the North Atlantic "conveyor belt" hypothesis for abrupt climate change. *Annu. Rev. Earth Planet. Sci.*, 35, s. 241-272.

Alley, R. B., Mayewski, P. A., Sowers, T., Stuiver, M., Taylor, K. C. & Clark, P. U. 1997. Holocene climatic instability: A prominent, widespread event 8200 yr ago. *Geology*, 25(6), s. 483-486.

Andreassen, K., Laberg, J. S. & Vorren, T. O. 2008. Seafloor geomorphology of the SW Barents Sea and its glaci-dynamic implications. *Geomorphology*, 97(1), s. 157-177.

Andreassen, K. & Winsborrow, M. 2009. Signature of ice streaming in Bjørnøyrenna, Polar North Atlantic, through the Pleistocene and implications for ice-stream dynamics. *Annals of Glaciology*, 50(52), s. 17-26.

Armstrong, H. A. & Brasier, M. D. 2005. Foraminifera. *Microfossils, Second Edition*, s. 142-187.

Bauch, H. A. 1994. Significance of variability in Turborotalita quinqueloba (Natland) test size and abundance for paleoceanographic interpretations in the Norwegian-Greenland Sea. *Marine Geology*, 121(1-2), s. 129-141.

Bauch, H. A., Erlenkeuser, H., Spielhagen, R. F., Struck, U., Matthiessen, J., Thiede, J. & Heinemeier, J. 2001. A multiproxy reconstruction of the evolution of deep and surface waters in the subarctic Nordic seas over the last 30,000 yr. *Quaternary Science Reviews*, 20(4), s. 659-678.

Bauch, H. A. & Weinelt, M. S. 1997. Surface water changes in the Norwegian Sea during last deglacial and Holocene times. *Quaternary Science Reviews*, 16(10), s. 1115-1124.

Bé, A. & Tolderlund, D. 1971. Distribution and ecology of living planktonic foraminifera in surface waters of the Atlantic and Indian Oceans. *The micropaleontology of oceans*, s. 105-149.

Benn, D. & Evans, D. 1998. Glaciers and glaciation: London. Arnold.

Berben, S. 2014. A Holocene palaeoceanographic multi-proxy study on the variability of Atlantic water inflow and sea ice distribution along the pathway of Atlantic water.

Blindheim, J. 1989. Cascading of Barents Sea bottom water into the Norwegian Sea. *Rapp. PV Reun. Cons. Int. Explor. Mer*, 188, s. 49-58.

Bond, G., Broecker, W., Johnsen, S., Mcmanus, J., Labeyrie, L., Jouzel, J. & Bonani, G. 1993. Correlations between climate records from North Atlantic sediments and Greenland ice. *Nature*, 365(6442), s. 143-147.

Bowman, S. 1990. *Interpreting the past: radiocarbon dating*. British Museum Publications.

Broecker, W. & Denton, G. 1990. What drives glacial cycles? *Scientific American*, 262(1), s. 43-50.

Carstens, J., Hebbeln, D. & Wefer, G. 1997. Distribution of planktic foraminifera at the ice margin in the Arctic (Fram Strait). *Marine Micropaleontology*, 29(3-4), s. 257-269.

Chauhan, T., Rasmussen, T., Noormets, R., Jakobsson, M. & Hogan, K. 2014. Glacial history and paleoceanography of the southern Yermak Plateau since 132 ka BP. *Quaternary Science Reviews*, 92, s. 155-169.

Corliss, B. H. 1985. Microhabitats of benthic foraminifera within deep-sea sediments.

Dahlgren, K. T., Vorren, T. O. & Laberg, J. S. 2002. Late Quaternary glacial development of the mid-Norwegian margin—65 to 68 N. *Marine and Petroleum Geology*, 19(9), s. 1089-1113.

De Schepper, G., Therrien, R., Refsgaard, J. C. & Hansen, A. L. 2015. Simulating coupled surface and subsurface water flow in a tile-drained agricultural catchment. *Journal of Hydrology*, 521, s. 374-388.

Deser, C., Walsh, J. E. & Timlin, M. S. 2000. Arctic sea ice variability in the context of recent atmospheric circulation trends. *Journal of Climate*, 13(3), s. 617-633.

Dokken, T. M. & Jansen, E. 1999. Rapid changes in the mechanism of ocean convection during the last glacial period. *Nature*, 401(6752), s. 458-461.

Doré, A. 1995. Barents Sea geology, petroleum resources and commercial potential. *Arctic*, s. 207-221.

Duplessy, J.-C., Moyes, J. & Pujol, C. 1980. Deep water formation in the North Atlantic Ocean during the last ice age. *Nature*, 286(5772), s. 479-482.

Duplessy, J. C., Ivanova, E., Murdmaa, I., Paterne, M. & Labeyrie, L. 2001. Holocene paleoceanography of the northern Barents Sea and variations of the northward heat transport by the Atlantic Ocean. *Boreas*, 30(1), s. 2-16.

Ebbesen, H. & Hald, M. 2004. Unstable younger dryas climate in the northeast North Atlantic. *Geology*, 32(8), s. 673-676.

Elverhøi, A., Svendsen, J. I., Solheim, A., Andersen, E. S., Milliman, J., Mangerud, J. & Hooke, R. L. 1995. Late Quaternary sediment yield from the high Arctic Svalbard area. *The Journal of Geology*, s. 1-17.

Ezat, M. M., Rasmussen, T. L. & Groeneveld, J. 2014. Persistent intermediate water warming during cold stadials in the southeastern Nordic seas during the past 65 ky. *Geology*, 42(8), s. 663-666.

Fairbanks, R. G. 1989. A 17, 000-year glacio-eustatic sea level record: influence of glacial melting rates on the Younger Dryas event and deep-ocean circulation. *Nature*, 342(6250), s. 637-642.

Faleide, J. I., Tsikalas, F., Breivik, A. J., Mjelde, R., Ritzmann, O., Engen, O., Wilson, J. & Eldholm, O. 2008. Structure and evolution of the continental margin off Norway and the Barents Sea. *Episodes*, 31(1), s. 82-91.

Faure, G. & Mensing, T. M. 2005. *Isotopes: principles and applications*. John Wiley & Sons Inc.

Foster, T. D. & Middleton, J. H. 1980. Bottom water formation in the western Weddell Sea. *Deep Sea Research Part A. Oceanographic Research Papers*, 27(5), s. 367-381. doi: http://dx.doi.org/10.1016/0198-0149(80)90032-1.

Godwin, H. 1962. Half-life of radiocarbon. *Nature*, 195.

Grant, K., Rohling, E., Bar-Matthews, M., Ayalon, A., Medina-Elizalde, M., Ramsey, C. B., Satow, C. & Roberts, A. 2012. Rapid coupling between ice volume and polar temperature over the past 150,000 [thinsp] years. *Nature*, 491(7426), s. 744-747.

Grootes, P., Stuiver, M., White, J., Johnsen, S. & Jouzel, J. 1993. Comparison of oxygen isotope records from the GISP2 and GRIP Greenland ice cores. *Nature*, 366(6455), s. 552-554.

Hald, M. 2001. Climate change and paleoceanography. *I*: *The Northern North Atlantic*. Springer, s. 281-290.

Hald, M., Andersson, C., Ebbesen, H., Jansen, E., Klitgaard-Kristensen, D., Risebrobakken, B., Salomonsen, G. R., Sarnthein, M., Sejrup, H. P. & Telford, R. J. 2007. Variations in temperature and extent of Atlantic Water in the northern North Atlantic during the Holocene. *Quaternary Science Reviews*, 26(25), s. 3423-3440.

Hald, M. & Aspeli, R. 1997. Rapid climatic shifts of the northern Norwegian Sea during the last deglaciation and the Holocene. *Boreas*, 26(1), s. 15-28.

Hald, M., Danielsen, T. K. & Lorentzen, S. 1989. Late Pleistocene - Holocene benthic foraminiferal distribution in the southwestern Barents Sea: Paleoenvironmental implications. *Boreas*, 18(4), s. 367-388.

Hald, M., Dokken, T. & Mikalsen, G. 2001. Abrupt climatic change during the last interglacial–glacial cycle in the polar North Atlantic. *Marine Geology*, 176(1), s. 121-137.

Hald, M. & Hagen, S. 1998. Early Preboreal cooling in the Nordic seas region triggered by meltwater. *Geology*, 26(7), s. 615-618.

Hald, M. & Korsun, S. 1997. Distribution of modern benthic foraminifera from fjords of Svalhard, European Arctic. *Journal of Foraminiferal Research*, 27, s. 101-122.

Hald, M. & Steinsund, P. I. 1992a. Distribution of surface sediment benthic foraminifera in the southwestern Barents Sea. *The Journal of Foraminiferal Research*, 22(4), s. 347-362.

Hald, M. & Steinsund, P. I. 1992b. Distribution of surface sediment benthic foraminifera in the southwestern Barents Sea. *Journal of Foraminiferal Research*, 22(4), s. 347-362.

Hjelstuen, B. O., Eldholm, O. & Faleide, J. I. 2007. Recurrent Pleistocene mega-failures on the SW Barents Sea margin. *Earth and Planetary Science Letters*, 258(3), s. 605-618.

Hopkins, T. S. 1991. The GIN Sea—A synthesis of its physical oceanography and literature review 1972–1985. *Earth-Science Reviews*, 30(3), s. 175-318.

Hunt, A. S. & Corliss, B. H. 1993. Distribution and microhabitats of living (stained) benthic foraminifera from the Canadian Arctic Archipelago. *Marine Micropaleontology*, 20(3-4), s. 321-345.

Husum, K. & Hald, M. 2004. A continuous marine record 8000-1600 cal. yr BP from the Malangenfjord, north Norway: foraminiferal and isotopic evidence. *The Holocene*, 14(6), s. 877-887.

Hüneke, H., Henrich, R., Hüneke, H. & Mulder, T. 2011. *Pelagic sedimentation in modern and ancient oceans*. Elsevier: Amsterdam, The Netherlands.

Hyvärinen, H. 1968. Late-Quaternary sediment cores from lakes on Bjørnøya. *Geografiska Annaler. Series A. Physical Geography*, s. 235-245.

Ingvaldsen, R. B. 2005. Width of the North Cape Current and location of the Polar Front in the western Barents Sea. *Geophysical Research Letters*, 32(16).

Jennings, A. E., Weiner, N. J., Helgadottir, G. & Andrews, J. T. 2004. Modern foraminiferal faunas of the southwestern to northern Iceland shelf: oceanographic and environmental controls. *Journal of Foraminiferal Research*, 34(3), s. 180-207.

Jessen, S. P., Rasmussen, T. L., Nielsen, T. & Solheim, A. 2010. A new Late Weichselian and Holocene marine chronology for the western Svalbard slope 30,000–0 cal years BP. *Quaternary Science Reviews*, 29(9–10), s. 1301-1312. doi: http://dx.doi.org/10.1016/j.quascirev.2010.02.020.

Johannessen, T., Jansen, E., Flatøy, A. & Ravelo, A. C. 1994. The relationship between surface water masses, oceanographic fronts and paleoclimatic proxies in surface

sediments of the Greenland, Iceland, Norwegian Seas. *I*: *Carbon cycling in the glacial ocean: constraints on the ocean's role in global change*. Springer, s. 61-85.

Junttila, J., Aagaard-Sørensen, S., Husum, K. & Hald, M. 2010. Late Glacial–Holocene clay minerals elucidating glacial history in the SW Barents Sea. *Marine Geology*, 276(1), s. 71-85.

Karpuz, N. K. & Jansen, E. 1992. A high‐resolution diatom record of the last deglaciation from the SE Norwegian Sea: Documentation of rapid climatic changes. *Paleoceanography*, 7(4), s. 499-520.

Katz, M. E., Cramer, B. S., Franzese, A., Hönisch, B., Miller, K. G., Rosenthal, Y. & Wright, J. D. 2010. Traditional and emerging geochemical proxies in foraminifera. *The Journal of Foraminiferal Research*, 40(2), s. 165-192.

Klitgaard Kristensen, D. & Sejrup, H. 1996. Modern benthic foraminiferal biofacies across the northern North Sea. *Sarsia*, 81(2), s. 97-106.

Knudsen, K. L. 1998. Foraminiferer i Kvartær stratigrafi: Laboratorie-og fremstillingsteknik samt udvalgte eksempler. *Geologisk Tidsskrift*, 3(125), s. 1-25.

Koç, N. & Jansen, E. 2002. Holocene climate evolution of the North Atlantic ocean and the Nordic Seas—A synthesis of new results. *I*: *Climate Development and History of the North Atlantic Realm*. Springer, s. 165-173.

Koç, N., Jansen, E. & Haflidason, H. 1993. Paleoceanographic reconstructions of surface ocean conditions in the Greenland, Iceland and Norwegian seas through the last 14 ka based on diatoms. *Quaternary Science Reviews*, 12(2), s. 115-140.

Kohfeld, K. E., Fairbanks, R. G., Smith, S. L. & Walsh, I. D. 1996. Neogloboquadrina pachyderma (sinistral coiling) as paleoceanographic tracers in polar oceans: Evidence from Northeast Water Polynya plankton tows, sediment traps, and surface sediments. *Paleoceanography*, 11(6), s. 679-699.

Korsun, S. & Hald, M. 1998. Modern benthic foraminifera off Novaya Zemlya tidewater glaciers, Russian Arctic. *Arctic and Alpine Research*, s. 61-77.

Korsun, S. & Hald, M. 2000. Seasonal dynamics of benthic foraminifera in a glacially fed fjord of Svalbard, European Arctic. *Journal of Foraminiferal Research*, 30(4), s. 251-271.

Laberg, J. & Vorren, T. 1993. A late Pleistocene submarine slide on the Bear Island trough mouth fan. *Geo-Marine Letters*, 13(4), s. 227-234.

Laberg, J. & Vorren, T. 1996. The middle and late pleistocence evolution and the bear island trough mouth fan. *Global and Planetary Change*, 12(1), s. 309-330.

Laberg, J. S., Stoker, M. S., Dahlgren, K. T., De Haas, H., Haflidason, H., Hjelstuen, B. O., Nielsen, T., Shannon, P. M., Vorren, T. O. & Van Weering, T. C. 2005. Cenozoic alongslope processes and sedimentation on the NW European Atlantic margin. *Marine and Petroleum Geology*, 22(9), s. 1069-1088.

Łącka, M., Zajączkowski, M., Forwick, M. & Szczuciński, W. 2015. Late Weichselian and Holocene palaeoceanography of Storfjordrenna, southern Svalbard.

Landvik, J. Y., Bondevik, S., Elverhoi, A., Fjeldskaar, W., Mangerud, J., Salvigsen, O., Siegert, M. J., Svendsen, J. I. & Vorren, T. O. 1998. The last glacial maximum of Svalbard and the Barents Sea area: Ice sheet extent and configuration. *Quaternary Science Reviews*, 17(1-3), s. 43-75. doi: 10.1016/s0277-3791(97)00066-8.

Lekens, W., Sejrup, H., Haflidason, H., Petersen, G., Hjelstuen, B. & Knorr, G. 2005. Laminated sediments preceding Heinrich event 1 in the Northern North Sea and Southern Norwegian Sea: origin, processes and regional linkage. *Marine Geology*, 216(1), s. 27-50.

Lind, S. & Ingvaldsen, R. B. 2012. Variability and impacts of Atlantic Water entering the Barents Sea from the north. *Deep Sea Research Part I: Oceanographic Research Papers*, 62, s. 70-88.

Linke, P. & Lutze, G. 1993a. Microhabitat preferences of benthic foraminifera—a static concept or a dynamic adaptation to optimize food acquisition? *Marine micropaleontology*, 20(3-4), s. 215-234.

Linke, P. & Lutze, G. F. 1993b. Microhabitat preferences of benthic foraminifera—a static concept or a dynamic adaptation to optimize food acquisition? *Marine micropaleontology*, 20(3-4), s. 215-234.

Mackensen, A. & Douglas, R. G. 1989. Down-core distribution of live and dead deep-water benthic foraminifera in box cores from the Weddell Sea and the California continental borderland. *Deep Sea Research Part A. Oceanographic Research Papers*, 36(6), s. 879-900. doi: http://dx.doi.org/10.1016/0198-0149(89)90034-4.

Mackensen, A., Grobe, H., Kuhn, G. & Fu¨Tterer, D. K. 1990. Benthic foraminiferal assemblages from the eastern Weddell Sea between 68 and 73°S: Distribution, ecology and fossilization potential. *Marine Micropaleontology*, 16(3), s. 241-283. doi: http://dx.doi.org/10.1016/0377-8398(90)90006-8.

Mackensen, A., Schmiedl, G., Harloff, J. & Giese, M. 1995. Deep-sea foraminifera in the South Atlantic Ocean: ecology and assemblage generation. *Micropaleontology*, s. 342-358.

Mackensen, A., Sejrup, H. P. & Jansen, E. 1985. The distribution of living benthic foraminifera on the continental slope and rise off southwest Norway. *Marine*

Micropaleontology, 9(4), s. 275-306. doi: http://dx.doi.org/10.1016/0377-8398(85)90001-5.

Mangerud, J. & Gulliksen, S. 1975. Apparent radiocarbon ages of recent marine shells from Norway, Spitsbergen, and Arctic Canada. *Quaternary Research*, 5(2), s. 263-273. doi: http://dx.doi.org/10.1016/0033-5894(75)90028-9.

Marcott, S. A., Clark, P. U., Padman, L., Klinkhammer, G. P., Springer, S. R., Liu, Z., Otto-Bliesner, B. L., Carlson, A. E., Ungerer, A. & Padman, J. 2011. Ice-shelf collapse from subsurface warming as a trigger for Heinrich events. *Proceedings of the National Academy of Sciences*, 108(33), s. 13415-13419.

Mead, G. A. & Kennett, J. P. 1987. The distribution of Recent benthic foraminifera in the Polar Front region, southwest Atlantic. *Marine Micropaleontology*, 11(4), s. 343-360. doi: http://dx.doi.org/10.1016/0377-8398(87)90006-5.

Murray, J. W. 1991. Ecology and distribution of benthic foraminifera. *Biology of Foraminifera. Academic Press, London*, s. 221-254.

Murray, J. W. 2006. *Ecology and applications of benthic foraminifera*. Cambridge University Press.

Müller, J. & Stein, R. 2014. High-resolution record of late glacial and deglacial sea ice changes in Fram Strait corroborates ice–ocean interactions during abrupt climate shifts. *Earth and Planetary Science Letters*, 403, s. 446-455.

Oliver, K. I., Hoogakker, B. A., Crowhurst, S., Henderson, G., Rickaby, R., Edwards, N. & Elderfield, H. 2010. A synthesis of marine sediment core δ 13 C data over the last 150 000 years. *Climate of the Past*, 6, s. 645-673.

Ottesen, D., Dowdeswell, J. & Rise, L. 2005. Submarine landforms and the reconstruction of fast-flowing ice streams within a large Quaternary ice sheet: The 2500-km-long Norwegian-Svalbard margin (57–80 N). *Geological Society of America Bulletin*, 117(7-8), s. 1033-1050.

Pausata, F. S., Li, C., Wettstein, J., Kageyama, M. & Nisancioglu, K. H. 2011. The key role of topography in altering North Atlantic atmospheric circulation during the last glacial period. *Past climate variability: model analysis and proxy intercomparison*.

Pfirman, S., Bauch, D. & Gammelsrød, T. 1994. The northern Barents Sea: water mass distribution and modification. *The polar oceans and their role in shaping the global environment*, s. 77-94.

Pflaumann, U., Sarnthein, M., Chapman, M., D'abreu, L., Funnell, B., Huels, M., Kiefer, T., Maslin, M., Schulz, H. & Swallow, J. 2003. Glacial North Atlantic: Sea‐surface conditions reconstructed by GLAMAP 2000. *Paleoceanography*, 18(3).

Polyak, L., Korsun, S., Febo, L. A., Stanovoy, V., Khusid, T., Hald, M., Paulsen, B. E. & Lubinski, D. J. 2002. Benthic foraminiferal assemblages from the southern Kara Sea, a river-influenced Arctic marine environment. *Journal of Foraminiferal Research*, 32(3), s. 252-273.

Poole, D. A., Skitem, J. & Vorren, T. O. 1994. Foraminiferal stratigraphy, palaeoenvironments and sedimentation of the glacigenic sequence southwest of Bjørrnøya. *Boreas*, 23(2), s. 122-138.

Quinn, R., Bull, J. & Dix, J. 1998. Optimal processing of marine high-resolution seismic reflection (Chirp) data. *Marine Geophysical Researches*, 20(1), s. 13-20.

Rasmussen, T. L. & Thomsen, E. 2004. The role of the North Atlantic Drift in the millennial timescale glacial climate fluctuations. *Palaeogeography, Palaeoclimatology, Palaeoecology*, 210(1), s. 101-116.

Rasmussen, T. L., Thomsen, E., Labeyrie, L. & Van Weering, T. C. 1996a. Circulation changes in the Faeroe-Shetland Channel correlating with cold events during the last glacial period (58–10 ka). *Geology*, 24(10), s. 937-940.

Rasmussen, T. L., Thomsen, E., Ślubowska, M. A., Jessen, S., Solheim, A. & Koç, N. 2007. Paleoceanographic evolution of the SW Svalbard margin (76 N) since 20,000 14 C yr BP. *Quaternary Research*, 67(1), s. 100-114.

Rasmussen, T. L., Thomsen, E., Weering, T. C. & Labeyrie, L. 1996b. Rapid changes in surface and deep water conditions at the Faeroe Margin during the last 58,000 years. *Paleoceanography*, 11(6), s. 757-771.

Rathburn, A. E. & Corliss, B. H. 1994. The ecology of living (stained) deep‐sea benthic foraminifera from the Sulu Sea. *Paleoceanography*, 9(1), s. 87-150.

Reynolds, L. & Thunell, R. C. 1985. Seasonal succession of planktonic foraminifera in the subpolar North Pacific. *Journal of Foraminiferal Research*, 15(4), s. 282-301.

Risebrobakken, B., Jansen, E., Andersson, C., Mjelde, E. & Hevrøy, K. 2003. A high‐resolution study of Holocene paleoclimatic and paleoceanographic changes in the Nordic Seas. *Paleoceanography*, 18(1).

Risebrobakken, B., Moros, M., Ivanova, E. V., Chistyakova, N. & Rosenberg, R. 2010. Climate and oceanographic variability in the SW Barents Sea during the Holocene. *The Holocene*.

Rüther, D. C., Bjarnadóttir, L. R., Junttila, J., Husum, K., Rasmussen, T. L., Lucchi, R. G. & Andreassen, K. 2012. Pattern and timing of the northwestern Barents Sea Ice Sheet deglaciation and indications of episodic Holocene deposition. *Boreas*, 41(3), s. 494-512.

Rüther, D. C., Mattingsdal, R., Andreassen, K., Forwick, M. & Husum, K. 2011. Seismic architecture and sedimentology of a major grounding zone system deposited by the Bjørnøyrenna Ice Stream during Late Weichselian deglaciation. *Quaternary Science Reviews*, 30(19), s. 2776-2792.

Saher, M., Kristensen, D. K., Hald, M., Pavlova, O. & Jørgensen, L. L. 2012. Changes in distribution of calcareous benthic foraminifera in the central Barents Sea between the periods 1965–1992 and 2005–2006. *Global and Planetary Change*, 98, s. 81-96.

Sarnthein, M., Jansen, E., Weinelt, M., Arnold, M., Duplessy, J. C., Erlenkeuser, H., Flatøy, A., Johannessen, G., Johannessen, T. & Jung, S. 1995. Variations in Atlantic surface ocean paleoceanography, 50° - 80° N: A time - slice record of the last 30,000 years. *Paleoceanography*, 10(6), s. 1063-1094.

Sarnthein, M., Kreveld, S., Erlenkeuser, H., Grootes, P., Kucera, M., Pflaumann, U. & Schulz, M. 2003. Centennial - to - millennial - scale periodicities of Holocene climate and sediment injections off the western Barents shelf, 75 N. *Boreas*, 32(3), s. 447-461.

Sarnthein, M., Stattegger, K., Dreger, D., Erlenkeuser, H., Grootes, P., Haupt, B. J., Jung, S., Kiefer, T., Kuhnt, W. & Pflaumann, U. 2001. Fundamental modes and abrupt changes in North Atlantic circulation and climate over the last 60 ky—concepts, reconstruction and numerical modeling. *I*: *The Northern North Atlantic*. Springer, s. 365-410.

Schock, S. G., Leblanc, L. R. & Mayer, L. A. 1989. Chirp subbottom profiler for quantitative sediment analysis. *Geophysics*, 54(4), s. 445-450.

Seidenkrantz, M.-S. 1995. Cassidulina teretis Tappan and Cassidulina neoteretis new species (Foraminifera): stratigraphic markers for deep sea and outer shelf areas. *Journal of Micropalaeontology*, 14(2), s. 145-157.

Sejrup, H., Birks, H., Kristensen, D. K. & Madsen, H. 2004. Benthonic foraminiferal distributions and quantitative transfer functions for the northwest European continental margin. *Marine Micropaleontology*, 53(1), s. 197-226.

Sejrup, H., Larsen, E., Landvik, J., King, E., Haflidason, H. & Nesje, A. 2000. Quaternary glaciations in southern Fennoscandia: evidence from southwestern Norway and the northern North Sea region. *Quaternary Science Reviews*, 19(7), s. 667-685.

Sejrup, H.-P. & Guilbault, J.-P. 1980. Cassidulina reniforme and C. obtusa (Foraminifera), taxonomy, distribution, and ecology. *Sarsia*, 65(2), s. 79-85.

Sejrup, H. P., Holtedahl, H., Norvik, O. & Miljeteig, I. 1980. Benthonic foraminifera as indicators of the paleoposition of the Subarctic Convergence in the Norwegian - Greenland Sea. *Boreas*, 9(3), s. 203-207.

Shackleton, N. 1987. Oxygen isotopes, ice volume and sea level. *Quaternary Science Reviews*, 6(3-4), s. 183-190.

Shackleton, N. J. 2000. The 100,000-year ice-age cycle identified and found to lag temperature, carbon dioxide, and orbital eccentricity. *Science*, 289(5486), s. 1897-1902.

Simstich, J., Sarnthein, M. & Erlenkeuser, H. 2003. Paired δ 18 O signals of Neogloboquadrina pachyderma (s) and Turborotalita quinqueloba show thermal stratification structure in Nordic Seas. *Marine Micropaleontology*, 48(1), s. 107-125.

Ślubowska, M. A., Koç, N., Rasmussen, T. L. & Klitgaard‐Kristensen, D. 2005. Changes in the flow of Atlantic water into the Arctic Ocean since the last deglaciation: evidence from the northern Svalbard continental margin, 80 N. *Paleoceanography*, 20(4).

Ślubowska-Woldengen, M., Koç, N., Rasmussen, T. L., Klitgaard-Kristensen, D., Hald, M. & Jennings, A. E. 2008. Time-slice reconstructions of ocean circulation changes on the continental shelf in the Nordic and Barents Seas during the last 16,000 cal yr BP. *Quaternary Science Reviews*, 27(15), s. 1476-1492.

Ślubowska-Woldengen, M., Rasmussen, T. L., Koc, N., Klitgaard-Kristensen, D., Nilsen, F. & Solheim, A. 2007. Advection of Atlantic Water to the western and northern Svalbard shelf since 17,500 calyr BP. *Quaternary Science Reviews*, 26(3), s. 463-478.

Spielhagen, R. F. & Erlenkeuser, H. 1994. Stable oxygen and carbon isotopes in planktic foraminifers from Arctic Ocean surface sediments: Reflection of the low salinity surface water layer. *Marine Geology*, 119(3), s. 227-250.

Steinsund, P., Polyak, L., Hald, M., Mikhailov, V. & Korsun, S. 1994. Distribution of calcareous benthic foraminifera in recent sediments of the Barents and Kara Sea. *Benthic Foraminifera in Surface Sediments of the Barents and Kara Seas: Modern and Late Quaternary Application. Ph. D. Thesis, Department of Geology, Institute of Biology and Geology, University of Tromsø, Norway*.

Steinsund, P. I. & Hald, M. 1994. Recent calcium carbonate dissolution in the Barents Sea: paleoceanographic applications. *Marine Geology*, 117(1-4), s. 303-316.

Streeter, S. S. 1973. Bottom water and benthonic foraminifera in the North Atlantic—Glacial-interglacial contrasts. *Quaternary Research*, 3(1), s. 131-141. doi: http://dx.doi.org/10.1016/0033-5894(73)90059-8.

Sun, X., Corliss, B. H., Brown, C. W. & Showers, W. J. 2006. The effect of primary productivity and seasonality on the distribution of deep-sea benthic foraminifera in the North Atlantic. *Deep Sea Research Part I: Oceanographic Research Papers*, 53(1), s. 28-47.

Svensson, A., Andersen, K. K., Bigler, M., Clausen, H. B., Dahl-Jensen, D., Davies, S., Johnsen, S. J., Muscheler, R., Parrenin, F. & Rasmussen, S. O. 2008. A 60 000 year Greenland stratigraphic ice core chronology. *Climate of the Past*, 4(1), s. 47-57.

Sztybor, K. & Rasmussen, T. L. 2016. Diagenetic disturbances of marine sedimentary records from methane‐influenced environments in the Fram Strait as indications of variation in seep intensity during the last 35 000 years. *Boreas*.

Sættem, J., Poole, D., Ellingsen, L. & Sejrup, H. 1992. Glacial geology of outer Bjørnøyrenna, southwestern Barents Sea. *Marine Geology*, 103(1), s. 15-51.

Tolderlund, D. S. & Bé, A. W. 1971. Seasonal distribution of planktonic foraminifera in the western North Atlantic. *Micropaleontology*, s. 297-329.

Vernal, A. D., Henry, M., Matthiessen, J., Mudie, P. J., Rochon, A., Boessenkool, K. P., Eynaud, F., Grøsfjeld, K., Guiot, J. & Hamel, D. 2001. Dinoflagellate cyst assemblages as tracers of sea-surface conditions in the northern North Atlantic, Arctic and sub-Arctic seas: the new'n= 677' data base and its application for quantitative palaeoceanographic reconstruction. *Journal of Quaternary Science*, 16(7), s. 681-698.

Vorren, T. O., Hald, M. & Lebesbye, E. 1988. Late cenozoic environments in the Barents Sea. *Paleoceanography*, 3(5), s. 601-612.

Vorren, T. O. & Kristoffersen, Y. 1986. Late Quaternary glaciation in the south‐western Barents Sea. *Boreas*, 15(1), s. 51-59.

Vorren, T. O. & Laberg, J. S. 1996. Late glacial air temperature, oceanographic and ice sheet interactions in the southern Barents Sea region. *Geological Society, London, Special Publications*, 111(1), s. 303-321.

Vorren, T. O. & Laberg, J. S. 1997. Trough mouth fans—palaeoclimate and ice-sheet monitors. *Quaternary Science Reviews*, 16(8), s. 865-881.

Vorren, T. O., Landvik, J. Y., Andreassen, K. & Laberg, J. S. 2011. Glacial history of the Barents Sea region. *Quaternary Glaciations—Extent and Chronology—A Closer Look, Dev. in Quat. Sci*, s. 361-372.

Vorren, T. O., Lebesbye, E. & Larsen, K. B. 1990. Geometry and genesis of the glacigenic sediments in the southern Barents Sea. *Geological Society, London, Special Publications*, 53(1), s. 269-288.

Vorren, T. O. & Plassen, L. 2002. Deglaciation and palaeoclimate of the Andfjord‐Vågsfjord area, North Norway. *Boreas*, 31(2), s. 97-125.

Waelbroeck, C., Duplessy, J.-C., Michel, E., Labeyrie, L., Paillard, D. & Duprat, J. 2001. The timing of the last deglaciation in North Atlantic climate records. *Nature*, 412(6848), s. 724-727.

Waelbroeck, C., Labeyrie, L., Michel, E., Duplessy, J. C., Mcmanus, J., Lambeck, K., Balbon, E. & Labracherie, M. 2002. Sea-level and deep water temperature changes derived from benthic foraminifera isotopic records. *Quaternary Science Reviews*, 21(1), s. 295-305.

Weber, M. E., Wiedicke, M. H., Kudrass, H. R., Hübscher, C. & Erlenkeuser, H. 1997. Active growth of the Bengal Fan during sea-level rise and highstand. *Geology*, 25(4), s. 315-318.

Winsborrow, M. C. M., Andreassen, K., Corner, G. D. & Laberg, J. S. 2010. Deglaciation of a marine-based ice sheet: Late Weichselian palaeo-ice dynamics and retreat in the southern Barents Sea reconstructed from onshore and offshore glacial geomorphology. *Quaternary Science Reviews*, 29(3–4), s. 424-442. doi: http://dx.doi.org/10.1016/j.quascirev.2009.10.001.

Wohlfarth, B., Lemdahl, G., Olsson, S., Persson, T., Snowball, I., Ising, J. & Jones, V. 1995. Early Holocene environment on Bjørnøya (Svalbard) inferred from multidisciplinary lake sediment studies. *Polar Research*, 14, s. 253-275.

Wollenburg, J. & Mackensen, A. 2009. The ecology and distribution of benthic foraminifera at the Håkon Mosby mud volcano (SW Barents Sea slope). *Deep Sea Research Part I: Oceanographic Research Papers*, 56(8), s. 1336-1370.

Wollenburg, J. E., Knies, J. & Mackensen, A. 2004. High-resolution paleoproductivity fluctuations during the past 24 kyr as indicated by benthic foraminifera in the marginal Arctic Ocean. *Palaeogeography, Palaeoclimatology, Palaeoecology*, 204(3), s. 209-238.

Wollenburg, J. E., Kuhnt, W. & Mackensen, A. 2001. Changes in Arctic Ocean paleoproductivity and hydrography during the last 145 kyr: the benthic foraminiferal record. *Paleoceanography*, 16(1), s. 65-77.

Wollenburg, J. E. & Mackensen, A. 1998. Living benthic foraminifers from the central Arctic Ocean: faunal composition, standing stock and diversity. *Marine Micropaleontology*, 34(3), s. 153-185.

Aagaard, K. & Greisman, P. 1975. Toward new mass and heat budgets for the Arctic Ocean. *Journal of Geophysical Research*, 80(27), s. 3821-3827.

Aagaard-Sørensen, S., Husum, K., Hald, M. & Knies, J. 2010. Paleoceanographic development in the SW Barents Sea during the late Weichselian–Early Holocene transition. *Quaternary Science Reviews*, 29(25), s. 3442-3456.

Aagaard-Sørensen, S., Husum, K., Werner, K., Spielhagen, R. F., Hald, M. & Marchitto, T. M. 2014. A Late Glacial–Early Holocene multiproxy record from the eastern Fram Strait, Polar North Atlantic. *Marine Geology*, 355, s. 15-26.